

Abstract

Determining the optimal distribution of flexural rigidity across a flapping plate to maximise thrust

by Dion Ho

In this paper, we will study flapping propulsion: e.g. a fish that propels itself through a fluid by waving its tail. An important question to ask is how to maximise the thrust generated by the flapping motion. One of the key parameters in the design of the tail – which we will model as a thin plate – is the distribution of rigidity across it. Our goal is to determine the optimal distribution to maximise thrust. We will present a unique approach to this problem, and our work complements earlier work done by Moore and Wu. In particular, we will solve for the kinematics of the tail/plate using the Unified Transform Method (UTM). Through this process, we will also facilitate the application of the UTM to physical problems.

Contents

Abstract	i
Acknowledgements	v
1 Introduction	1
1.1 Preliminary discussion and literature review	2
1.1.1 Wu’s fluid flow analysis	3
1.1.2 Moore’s numerics and hypothesis	5
1.1.3 The Unified Transform Method (UTM)	6
2 Solving for the Kinematics	8
2.1 Problem setup	8
2.2 Stage 1	9
2.3 Stage 2	17
2.3.1 Demonstrating zero contribution from each integral that contains \hat{g} and \hat{h}	27
2.3.2 Justifying the removal of the open discs	36
3 Further Analysis	38

List of Tables

2.1	The asymptotic behaviour of basic exponential functions as $k \rightarrow \infty$ in a subset of each quadrant of \mathbb{C}	32
-----	--	----

List of Figures

1.1	An illustration of our fish tail model and its kinematics. The kinematics shown are for illustrative purposes only and are not mathematically accurate.	2
2.1	An illustration of the four regions defined by (2.2.8). They each correspond to a quadrant of \mathbb{C} . The circles are created by the open discs we removed from \mathcal{D}_m^\pm . While the illustration of the circles is in general not mathematically accurate, we will define Ξ such that the circles have 4-fold rotational symmetry about the origin.	15
2.2	Each colour indicates a set of conjugate powers collected from $\Delta_1(k)$ (top) or $\Delta_2(k)$ (bottom), after cancellation with the numerator, for particular values of S_1/S_2 and L . Observe that the convex hull for each of these sets of points is rectangular. The points in grey show the conjugate powers for $S_1/S_2 \in [0.2, 5]$ and $L \in (-1, 1)$	37

Acknowledgements

A massive thank you to my advisor Professor David Smith for all his advice, help and support.

To my family, my girlfriend, and all my other friends, thank you for putting up with me as I slogged through my capstone. Your encouragement and support has been invaluable < 3

Chapter 1

Introduction

Consider a fish that propels itself through a fluid by waving its tail. Suppose the movement of the tail is two-dimensional with the length of the tail as the x -axis and the y -axis defined to be perpendicular to it. If we simplify the tail to be a plate of negligible thickness and view it in the plane of its movement, it can be modelled as a one-dimensional beam (see Figure 1.1).

The movement/kinematics of the beam is governed by the Euler-Bernoulli dynamic beam equation (see [4] for its derivation and properties):

$$\frac{\partial^2 h}{\partial t^2} + \mu \frac{\partial^2}{\partial x^2} \left(S(x) \frac{\partial^2 h}{\partial x^2} \right) = p(x, t), \quad (1.0.1)$$

where $\mu > 0$ is the constant mass per unit length, $S(x) > 0$ is the flexural rigidity of the beam, and $p(x, t)$ is the net pressure exerted on the beam (per unit length) by the surrounding fluid. The movement of the plate affects the surrounding fluid in such a way as to generate thrust. Thus, if we know both the kinematics of the beam and the surrounding fluid flow, we can calculate the thrust generated by the waving plate. The overarching goal of this capstone project is to determine the optimal distribution of flexural rigidity (henceforth shortened to “rigidity”) across a flapping plate to maximise thrust. We hope that our results will benefit the engineering

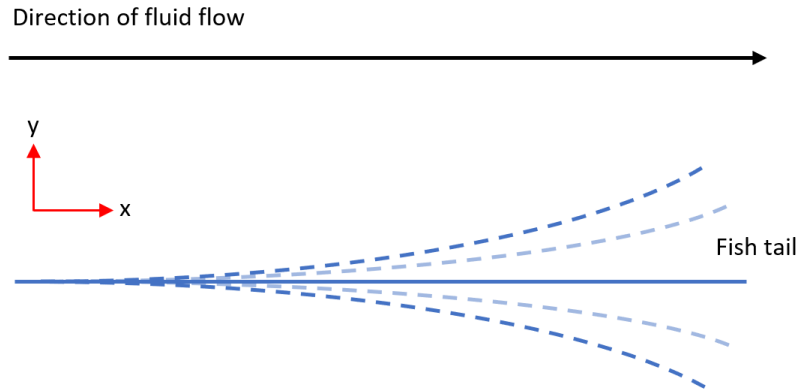


FIGURE 1.1: An illustration of our fish tail model and its kinematics. The kinematics shown are for illustrative purposes only and are not mathematically accurate.

of propulsive devices like swimming fins or flapping foils (see [1] for a fascinating discussion of flapping foil propulsion systems). Our results may also be useful in biomimicry and aquatic evolutionary biology.

1.1 Preliminary discussion and literature review

On the surface, (1.0.1) appears to be a standard inhomogeneous beam equation. If standard boundary and initial conditions are specified, we get an initial boundary value problem (IBVP) that is difficult to solve due to the fourth order partial differential equation (PDE), but is well-studied. The additional complication in our case is that $p(x, t)$ is dependent on $h(x, t)$: we need to solve PDEs involving $h(x, t)$ to determine $p(x, t)$. Consider the underlying physics: we would expect the kinematics of the beam to be affected by the pressure exerted on it by the surrounding fluid. The pressure, in turn, is determined by the fluid flow around the beam. Yet, the fluid

flow is itself affected by the kinematics of the beam. Thus, we have a mutually dependent system. In order to properly solve for both the kinematics and the fluid flow, we need to solve a system of complicated PDEs which includes (1.0.1). The full problem, without any major simplifying assumptions, likely remains analytically intractable. In the proceeding literature review, we will discuss Moore's [12, 13] and Wu's [16] work on the problem, and highlight the gaps that remain. Our work will help to fill in these gaps and bring us closer to a complete solution of the problem.

1.1.1 Wu's fluid flow analysis

In [16], Wu starts with the assumption that the kinematics $h(x, t)$ are known. From our discussion above, it is clear that this assumption is a contrivance, and it prevents Wu's results from being of practical use. Nonetheless, this assumption allows Wu to produce a number of important analytical results regarding the fluid flow. We will reproduce some of [16, pp. 321–324] to explicate how the fluid flow, and in turn the pressure, is affected by the kinematics of the beam. The fluid flow is not the focus for our present work though; the reader is referred to [16] for more details.

Wu's starting point for his fluid flow analysis is the flow velocity vector $\vec{q} =$ with (x, y) components $(U + u, v)$. The undisturbed velocity of the stream, which is assumed to be initially uniform, is $(U, 0)$ with $U > 0$. The perturbation of the stream is given by the vector (u, v) . The flow velocity satisfies the continuity equation $\nabla \cdot \vec{q} = u_x + v_y = 0$. Wu assumes that $u, v \ll U$ and uses the linearised Euler ideal fluid equations to get

$$\left(\frac{\partial}{\partial t} + U \frac{\partial}{\partial x} \right) \vec{q} = \nabla \phi(x, y, t),$$

where ϕ is Prandtl's acceleration potential. Importantly, the term $p(x, t)$ which appears in (1.0.1) is given by

$$p(x, t) = \rho(\phi(x, 0^+, t) - \phi(x, 0^-, t)),$$

for ρ the density of the fluid. This equation relates the pressure exerted on the beam to the acceleration potential and tells us that the net pressure is the difference in the pressure exerted on the top and bottom of the beam. Wu shows that ϕ is a harmonic function and defines its harmonic conjugate as ψ with $\phi_x = \psi_y$ and $\phi_y = -\psi_x$. Consequently, Wu derives the relation between the kinematics of the beam and the acceleration potential on its top and bottom surfaces as

$$\phi_y = -\psi_x = \left(\frac{\partial}{\partial t} + U \frac{\partial}{\partial x} \right)^2 h \text{ on } y = \pm 0.$$

In addition, Wu gives the formula for thrust (in the x -direction) as

$$T = \int_X \operatorname{Re}(p(x, t)) \operatorname{Re}(h_x(x, t)) dx + T_s,$$

where X is domain of the beam, the first term is the thrust due to the net pressure on the beam, denoted T_p , and the second term is the thrust due to leading-edge suction (there is a flow singularity at the leading edge). T_s can be calculated from the kinematics and pressure as well, though less directly. Moore discusses the calculation of thrust in further detail in [12, p. 611]. In practice there will also be a drag term, which has dependence on the velocity and the kinematics, acting against the thrust.

In summary, if the kinematics of the beam and the net pressure exerted

on it are known, then the thrust generated by the flapping plate can be determined. Wu made two major assumptions though. The first, as previously discussed, is that the kinematics are known. The second assumption, which is also used by Moore, is that the kinematics are simple harmonic. This second assumption is common in physics and it is partly justified by Wu's assumption that the amplitude of h and h_x are small. Note too that the Euler-Bernoulli beam equation is only valid for small deflections. Nonetheless, it remains an open question as to whether the actual kinematics can be well-approximated as simple harmonic motion. We will attempt to answer this question in our present work.

1.1.2 Moore's numerics and hypothesis

Moore provides two approaches to solving the full problem. Both approaches amount to simplifying the kinematics sufficiently that the full problem can be solved either analytically [12] or numerically [13].

In [12], Moore assumes a torsional spring model for simple harmonic kinematics to derive $h(x, t) = (\beta_0/2 + \beta_1) e^{j\omega t}$, where β_0, β_1 are to be determined. Physically, the model represents a rigid beam attached to a driver at the leading edge through a torsional spring. Moore argues that this model approximates a concentration of flexibility at the leading edge; we can think of the rigidity function $S(x)$ in (1.0.1) being small at the leading edge and large everywhere else. Using this assumption and building on Wu's work, Moore is able to analytically solve for both the kinematics and pressure.

In [13], Moore uses the beam equation (1.0.1) and again assumes the kinematics to be simple harmonic. This implies that $h_{tt} = -Fh$, where $F > 0$, and $h(x) = \eta(x)e^{j\omega t}$ (j is the imaginary constant). Consequently,

he simplifies (1.0.1) to the ordinary differential equation (ODE):

$$\mu \frac{\partial^2}{\partial x^2} \left(S(x) \frac{\partial^2 h}{\partial x^2} \right) - Fh = p(x, t),$$

which is [13, equation (7)], though with different constants. Even with this simplification, the resultant system is analytically intractable. Thus, Moore uses a numerical method: Chebyshev collocation with GMRES to solve it for the kinematics, pressure, and consequently thrust. In addition, Moore numerically optimised the thrust over uniform, linear, quadratic, and cubic distributions of $S(x)$ (see [13, p. 4] for more details). Moore's results indicate that, for a fixed driving force, thrust is maximised when the flexibility of the beam is concentrated at its leading edge. His ostensible limit case, the torsional spring model, produces the most thrust. Moore's findings provide a hypothetical answer to the overarching problem. Unfortunately, since Moore's approach is numerical, the findings are unproven. In addition, Moore, like Wu, relied greatly upon the assumption that the kinematics are simple harmonic, but the extent to which this is true is unclear. Thus, our primary objective will be to rigorously analyse the kinematics of the beam. Our work will, in a sense, be the opposite of Wu's work: he assumes the kinematics are known and solves for the fluid flow/pressure, we will assume that the pressure is known and solve for the kinematics.

1.1.3 The Unified Transform Method (UTM)

We will use the three-stage Unified Transform Method (UTM), also known as the Fokas method, to solve for the kinematics. The UTM is a powerful and relatively new PDE solving method that can solve most linear PDEs

and even some non-linear PDEs. It was first presented by Fokas in 1997 [5]. Miller and Smith provide a comprehensive overview of the UTM, together with a summary of its history, in [11, §2]. Recently, in 2018, Deconinck et al. [3] developed a variant of the UTM to address equations of the form

$$Q_t + \Lambda(k)Q = 0, \quad k := -i\partial_x$$

where Q is an N -dimensional vector and Λ is a matrix-valued polynomial of size $N \times N$ and order n ; for the wave and beam equations, $n = 2$. Their paper built upon the work of Fokas and Pelloni in [6]. Given the recency of Deconinck's UTM variant, we are, as far as we know, the first to apply it to the beam equation. Even the UTM cannot solve the beam equation with a continuous distribution of rigidity $S(x)$ though. Therefore, we will instead consider a piecewise constant $S(x)$. This leads to an interface problem. The UTM has been successfully applied to interface problems, though only for equations that are first-order in time [2, 15]. Increasing the number of pieces in $S(x)$ will allow it to better approximate continuous functions.

Although the UTM is in theory a very powerful PDE solving tool, there are practical concerns inherent to the solving of high order PDE problems. In particular, the resultant solution representation tends to be extremely long. This is especially true when the spatial domain is a finite interval since there are two boundary conditions to address. In [15], for example, Sheils and Deconinck used the UTM to solve the zero potential linear Schrodinger equation initial interface value problem (IIVP) on a finite interval. Their full solution representation spans two and a half pages [15, pp. 270–273]. Thus, our secondary objective is to address these practical concerns with regard to the UTM and facilitate its practical application.

Chapter 2

Solving for the Kinematics

2.1 Problem setup

We begin by specifying the full beam equation IIVP that we wish to solve:

$$\frac{\partial^2 h}{\partial t^2} + \mu \frac{\partial^2 h}{\partial x^2} \left(S(x) \frac{\partial^2 h}{\partial x^2} \right) = p(x, t), \quad (x, t) \in (-1, 1) \times (0, \mathcal{T}), \quad (2.1.1)$$

with $\mu, S(x) > 0$. The time domain is finite, though an infinite domain will not change our solution. We set up an interface by making $S(x)$ piecewise constant,

$$S(x) = \begin{cases} S_1, & x \in [-1, L], \\ S_2, & x \in (L, 1], \end{cases}$$

where $S_1 \ll S_2$, $L \in (-1, 1)$, and we will consider the limit $L \rightarrow -1$. At the interface we have equality up to and including the third spatial derivative. The initial conditions are $h(x, 0) = h_0(x)$ and $h_t(x, 0) = g_0(x)$.

The boundary conditions are

$$\begin{aligned} h(-1, t) &= A \cos(\omega t), & h_x(-1, t) &= 0, \\ h_{xx}(1, t) &= 0, & h_{xxx}(1, t) &= 0, \end{aligned} \quad (2.1.2)$$

for some frequency ω and amplitude A . We assume that the initial conditions fulfil the boundary conditions and that $p(x, t)$ is integrable.

Our boundary conditions are taken directly from Moore [13, p. 3]. Physically, $h_x(-1, t) = 0$ and $h(-1, t) = A \cos(\omega t)$ model the left end of the beam being clamped to a body/driver which motion is simple harmonic. The body supplies a pure heaving force to the beam. Instead of $h_x(-1, t) = 0$, we could have chosen $h_{xx}(-1, t) = 0$, which implies zero curvature and models a pivot at $x = -1$. This would represent a pure pitching driving force. We can also choose $\alpha h_x(-1, t) + \beta h_{xx}(-1, t) = 0$ to represent a driving force that is part heaving and part pitching. For our right boundary conditions to imply a free end, we need the beam at $x = 1$ to have zero curvature and zero shear. Thus, we use $h_{xx}(1, t)$ (curvature) = $h_{xxx}(1, t)$ (shear) = 0. Further physical justification can be found in [4, §4.3] and [7, pp. 940–941].

2.2 Stage 1

We will mostly follow Stage 1 of the UTM in [3]¹. Since Deconinck [3] only addresses homogeneous PDEs, we will have to adapt his UTM variant to our inhomogeneous PDE. We begin by decomposing (2.1.1) into two systems

$$h_t = g, \quad g_t = -\mu S_n h_{xxxx} + p(x, t), \quad n(x) = 1, 2, \quad (2.2.1)$$

which correspond to each sub-interval. We assume that the IIVP, and by extension the systems (2.2.1), have a solution. This is usually justified in Stage 3 through verifying that the final solution representation satisfies the problem. In our case, we can be confident, a priori, that this assumption of

¹We used a Python-based computer algebra system called SymPy for verification. The Jupyter Notebook can be found here: <https://tinyurl.com/capstoneDH>.

solvability holds given the physical context from which the problem arose. Consequently, we will omit Stage 3. Re-express the systems (2.2.1) as

$$Q_t + \Lambda_n(-i\partial_x)Q = \rho, \quad Q = \begin{pmatrix} h \\ g \end{pmatrix}, \quad \Lambda_n(k) = \begin{pmatrix} 0 & -1 \\ \mu S_n k^4 & 0 \end{pmatrix}, \quad \rho = \begin{pmatrix} 0 \\ p \end{pmatrix}, \quad (2.2.2)$$

for $k \in \mathbb{C}$. The right-hand side of (2.2.2) is non-zero because our PDE is inhomogeneous. The eigenvalues of $\Lambda_n(k)$ are

$$\Omega_n^{(1)} = ik^2 \sqrt{\mu S_n}, \quad \Omega_n^{(2)} = -ik^2 \sqrt{\mu S_n}. \quad (2.2.3)$$

We drop the explicit k -dependence of the eigenvalues for simplicity of notation, though we will keep the k -dependence of functions that include the eigenvalues. Importantly, these eigenvalues do not have branch points. If they did, this approach would be significantly more complicated. A discussion of branch points and how to address them may be found in [3]. Since $\mu, S_n > 0$, the eigenvalues are distinct and $\Lambda_n(k)$ may be diagonalised as

$$\Lambda_n(k) = A_n^{-1}(k)D_n(k)A_n(k), \quad D_n(k) = \text{diag}(\Omega_n^{(1)}, \Omega_n^{(2)}),$$

for some matrix $A_n(k)$. Consequently, (2.2.2) can be expressed as

$$\left(e^{-ikxI + D_n(k)t} A_n(k) Q \right)_t - \left(e^{-ikxI + D_n(k)t} A_n(k) X_n(x, t, k) \right)_x = 0, \quad (2.2.4)$$

where $X_n(x, t, k)$ incorporates the inhomogeneity $p(x, t)$:

$$X_n(x, t, k) = i \left(\frac{\Lambda_n(k) - \Lambda_n(-i\partial_x)}{k - (-i\partial_x)} \right) Q + i(k - (-i\partial_x))^{-1} \rho.$$

Proof. Our proof for the form of $X_n(x, t, k)$ follows a similar proof in [6, p. 88]. First, perform the differentiations in (2.2.4) to get

$$\begin{aligned} & D_n(k)e^{-ikxI+D_n(k)t}A_n(k)Q + e^{-ikxI+D_n(k)t}A_n(k)Q_t \\ & - \left(-ike^{-ikxI+D_n(k)t}A_n(k)X_n(x, t, k) + e^{-ikxI+D_n(k)t}A_n(k)\partial_x X_n(x, t, k)\right) = 0. \end{aligned}$$

Using (2.2.2), we substitute Q_t with $-\Lambda_n(-i\partial_x)Q + \rho$ to get

$$\begin{aligned} & D_n(k)e^{-ikxI+D_n(k)t}A_n(k)Q + e^{-ikxI+D_n(k)t}A_n(k)(-\Lambda_n(-i\partial_x)Q + \rho) \\ & - \left(-ike^{-ikxI+D_n(k)t}A_n(k)X_n(x, t, k) + e^{-ikxI+D_n(k)t}A_n(k)\partial_x X_n(x, t, k)\right) = 0, \end{aligned}$$

where $D_n(k)$ and $e^{-ikxI+D_n(k)t}$ are diagonal matrices, which commute. Premultiply by $A_n^{-1}(k)e^{-(ikxI+D_n(k)t)}$ to get

$$\begin{aligned} & A_n^{-1}(k)D_n(k)A_n(k)Q - \Lambda_n(-i\partial_x)Q + \rho \\ & - (-ikX_n(x, t, k) + \partial_x X_n(x, t, k)) = 0 \\ \implies & \Lambda_n(k)Q - \Lambda_n(-i\partial_x)Q + \rho - (-ikX_n(x, t, k) + \partial_x X_n(x, t, k)) = 0 \\ \implies & (\Lambda_n(k) - \Lambda_n(-i\partial_x))Q + \rho = (-ik + \partial_x)X_n(x, t, k) \\ \implies & X_n(x, t, k) = \left(\frac{\Lambda_n(k) - \Lambda_n(-i\partial_x)}{-ik + \partial_x}\right)Q + (-ik + \partial_x)^{-1}\rho \\ \implies & X_n(x, t, k) = i\left(\frac{\Lambda_n(k) - \Lambda_n(-i\partial_x)}{k - (-i\partial_x)}\right)Q + i(k - (-i\partial_x))^{-1}\rho \end{aligned}$$

which is the desired form. \square

Consequently, we have

$$A_n(k) = \begin{pmatrix} \Omega_n^{(1)} & -1 \\ \Omega_n^{(2)} & -1 \end{pmatrix}, \quad X_n(x, t, k) = \begin{pmatrix} c_1(t)e^{ikx} \\ \mu S_n(k^3 - ik^2\partial_x - k\partial_x^2 + i\partial_x^3)h + iP \end{pmatrix},$$

where $(k + i\partial_x)P(x, t) = p(x, t)$ which is equivalent to

$$P(x, t) = e^{ikx} \left(\int_{-1}^x -ip(y, t)e^{-iky} dy + c_2(t) \right).$$

The terms $c_1(t)e^{ikx}$ and $c_2(t)e^{ikx}$ will vanish when substituted into (2.2.4).

Thus, we can set $c_1(t) \equiv c_2(t) \equiv 0$. Each system in (2.2.4) can be decoupled to form two equations

$$\begin{aligned} & \left(e^{-ikx + \Omega_n^{(m)}t} (\Omega_n^{(m)}h - g) \right)_t \\ & + \left(e^{-ikx + \Omega_n^{(m)}t} (\mu S_n (k^3h - ik^2h_x - kh_{xx} + ih_{xxx}) + iP) \right)_x = 0, \end{aligned}$$

for $m = 1, 2$. In UTM literature, these equations are called the local relations. The IIVP has two sets of local relations corresponding to each sub-interval and indexed by n .

Next, we integrate each local relation in each set over its respective space-time rectangle $(-1, L) \times (0, t)$ or $(L, 1) \times (0, t)$. The local relations are in divergence form: $\psi_t - \varphi_x = 0$. Therefore, we can apply Green's theorem to get a set of global relations for each sub-interval. For $m = 1, 2$:

$$\begin{aligned} & \left(\Omega_1^{(m)}\hat{h}_0 - \hat{g}_0 \right)(k; 1) + e^{\Omega_1^{(m)}t} \left(\hat{g} - \Omega_1^{(m)}\hat{h} \right)(k; t; 1) \\ & + e^{ik} \left(\mu S_1 \left(k^3u_0^{(m)} - ik^2u_1^{(m)} - ku_2^{(m)} + iu_3^{(m)} \right) + i\tilde{P}^{(m)} \right)(k; t; 1, -1) \\ & - e^{-iLk} \left(\mu S_1 \left(k^3u_0^{(m)} - ik^2u_1^{(m)} - ku_2^{(m)} + iu_3^{(m)} \right) + i\tilde{P}^{(m)} \right)(k; t; 1, L) = 0, \quad n(x) = 1, \\ & \left(\Omega_2^{(m)}\hat{h}_0 - \hat{g}_0 \right)(k; 2) + e^{\Omega_2^{(m)}t} \left(\hat{g} - \Omega_2^{(m)}\hat{h} \right)(k; t; 2) \\ & + e^{-iLk} \left(\mu S_2 \left(k^3u_0^{(m)} - ik^2u_1^{(m)} - ku_2^{(m)} + iu_3^{(m)} \right) + i\tilde{P}^{(m)} \right)(k; t; 2, L) \\ & - e^{-ik} \left(\mu S_2 \left(k^3u_0^{(m)} - ik^2u_1^{(m)} - ku_2^{(m)} + iu_3^{(m)} \right) + i\tilde{P}^{(m)} \right)(k; t; 2, 1) = 0, \quad n(x) = 2. \end{aligned} \tag{2.2.5}$$

The global relations are valid for all $k \in \mathbb{C}$. Note that L should more accurately be written as L^- (left limit), for $n(x) = 1$, and L^+ (right limit), for $n(x) = 2$. The distinction is irrelevant only because we have equality up to and including the third spatial derivative at the interface. The denotations used in the global relations are

$$\begin{aligned} \hat{h}_0(k; 1) &= \int_{-1}^L e^{-ikx} h_0(x) dx, & \hat{g}_0(k; 1) &= \int_{-1}^L e^{-ikx} g_0(x) dx, \\ \hat{h}(k; t; 1) &= \int_{-1}^L e^{-ikx} h(x, t) dx, & \hat{g}(k; t; 1) &= \int_{-1}^L e^{-ikx} g(x, t) dx, \\ \hat{h}_0(k; 2) &= \int_L^1 e^{-ikx} h_0(x) dx, & \hat{g}_0(k; 2) &= \int_L^1 e^{-ikx} g_0(x) dx, \\ \hat{h}(k; t; 2) &= \int_L^1 e^{-ikx} h(x, t) dx, & \hat{g}(k; t; 2) &= \int_L^1 e^{-ikx} g(x, t) dx, \end{aligned} \quad (2.2.6a)$$

and

$$\begin{aligned} u_0^{(m)}(k; t; n, \lambda) &= \int_0^t e^{\Omega_n^{(m)} s} h(\lambda, s) ds, & u_1^{(m)}(k; t; n, \lambda) &= \int_0^t e^{\Omega_n^{(m)} s} h_x(\lambda, s) ds, \\ u_2^{(m)}(k; t; n, \lambda) &= \int_0^t e^{\Omega_n^{(m)} s} h_{xx}(\lambda, s) ds, & u_3^{(m)}(k; t; n, \lambda) &= \int_0^t e^{\Omega_n^{(m)} s} h_{xxx}(\lambda, s) ds, \\ \tilde{P}^{(m)}(k; t; n, \lambda) &= \int_0^t e^{\Omega_n^{(m)} s} P(\lambda, s) ds. \end{aligned} \quad (2.2.6b)$$

For each sub-interval, we use the two global relations (2.2.5) to eliminate \hat{g} , then make \hat{h} the subject. Next, we apply the inverse Fourier transform so that \hat{h} is transformed to $2\pi h$. We obtain

$$2\pi h(x, t) =$$

$$\begin{cases} T_1(x, t; 1) + T_2^{(2)}(x, t; 1) - T_2^{(1)}(x, t; 1) - T_3^{(2)}(x, t; 1) + T_3^{(1)}(x, t; 1), & x \in (-1, L], \\ T_1(x, t; 2) + T_3^{(2)}(x, t; 2) - T_3^{(1)}(x, t; 2) - T_4^{(2)}(x, t; 2) + T_4^{(1)}(x, t; 2), & x \in (L, 1), \end{cases}$$

where

$$\begin{aligned}
T_1(x, t; n) &= \int_{-\infty}^{\infty} e^{ikx} \frac{\left(e^{-\Omega_n^{(2)}t} \left(\Omega_n^{(2)} \hat{h}_0 - \hat{g}_0 \right) - e^{-\Omega_n^{(1)}t} \left(\Omega_n^{(1)} \hat{h}_0 - \hat{g}_0 \right) \right) (k; n)}{\Omega_n^{(2)} - \Omega_n^{(1)}} dk, \\
T_2^{(m)}(x, t; 1) &= \int_{-\infty}^{\infty} e^{ik(x+1) - \Omega_1^{(m)}t} \\
&\quad \left[\frac{\left(\mu S_1 \left(k^3 u_0^{(m)} - ik^2 u_1^{(m)} - k u_2^{(m)} + i u_3^{(m)} \right) + i \tilde{P}^{(m)} \right) (k; t; 1, -1)}{\Omega_1^{(2)} - \Omega_1^{(1)}} \right] dk, \\
T_3^{(m)}(x, t; n) &= \int_{-\infty}^{\infty} e^{ik(x-L) - \Omega_n^{(m)}t} \\
&\quad \left[\frac{\left(\mu S_n \left(k^3 u_0^{(m)} - ik^2 u_1^{(m)} - k u_2^{(m)} + i u_3^{(m)} \right) + i \tilde{P}^{(m)} \right) (k; t; n, L)}{\Omega_n^{(2)} - \Omega_n^{(1)}} \right] dk, \\
T_4^{(m)}(x, t; 2) &= \int_{-\infty}^{\infty} e^{ik(x-1) - \Omega_2^{(m)}t} \\
&\quad \left[\frac{\left(\mu S_2 \left(k^3 u_0^{(m)} - ik^2 u_1^{(m)} - k u_2^{(m)} + i u_3^{(m)} \right) + i \tilde{P}^{(m)} \right) (k; t; 2, 1)}{\Omega_2^{(2)} - \Omega_2^{(1)}} \right] dk.
\end{aligned} \tag{2.2.7}$$

In this preliminary solution representation, both T_1 are known and no further manipulation is necessary. Initially, each of $\left(T_2^{(2)} - T_2^{(1)}\right)$, $\left(T_3^{(2)} - T_3^{(1)}\right)$ and $\left(T_4^{(2)} - T_4^{(1)}\right)$ were combined. We can distribute these integrals without concern because our eigenvalues have no branch points, and this is done to prepare for the deformation of integration contours.

Standard UTM procedure requires that we deform the integration contour of every term except T_1 . We will make use of these deformations at the end of Stage 2, in §2.3.1. We first define the regions

$$\mathcal{D}_m^\pm = \{k \in \mathbb{C}^\pm : \operatorname{Re}(\Omega_n^{(m)}) < 0\}, \quad D_m^\pm = \mathcal{D}_m^\pm \setminus \bigcup_{\xi \in \Xi} R(\xi, M). \tag{2.2.8}$$

The regions are independent of index n and correspond to the quadrants of

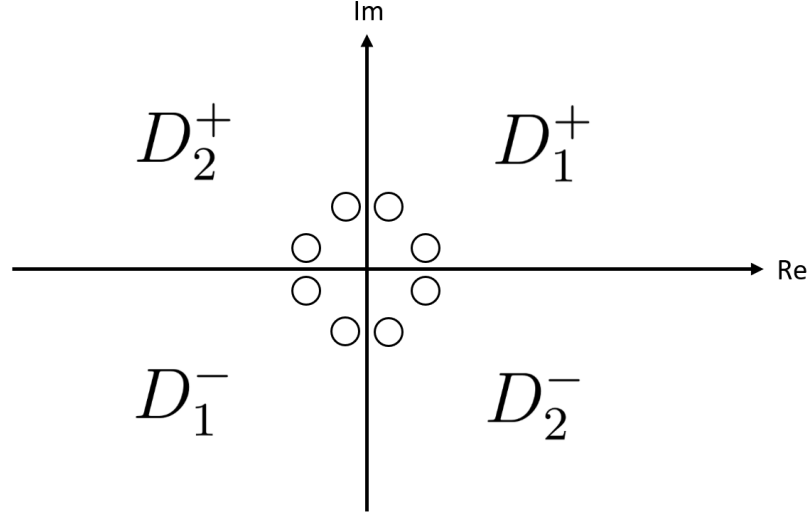


FIGURE 2.1: An illustration of the four regions defined by (2.2.8). They each correspond to a quadrant of \mathbb{C} . The circles are created by the open discs we removed from \mathcal{D}_m^\pm . While the illustration of the circles is in general not mathematically accurate, we will define Ξ such that the circles have 4-fold rotational symmetry about the origin.

\mathbb{C} . The boundaries $\partial\mathcal{D}_m^\pm$ and ∂D_m^\pm are oriented in the positive sense. The set Ξ contains the zeros of some functions, and each $R(\xi, M)$ is an open disc with a small radius M centered on a zero ξ (these are discussed in §2.3.1 and §2.3.2). Figure 2.1 provides an illustration of the regions D_m^\pm .

From (2.2.6b), the spectral inhomogeneities $\tilde{P}^{(m)}$ and spectral functions $u_0^{(m)}, u_1^{(m)}, u_2^{(m)}, u_3^{(m)}$ multiplied by $e^{-\Omega_n^{(m)}t}$ each has the form

$$\int_0^t e^{\Omega_n^{(m)}(s-t)} \phi(\lambda, s) ds.$$

Integration by parts gives

$$\begin{aligned} \int_0^t e^{\Omega_n^{(m)}(s-t)} \phi(\lambda, s) ds &= \frac{1}{\Omega_n^{(m)}} \left(\phi(\lambda, t) - e^{-\Omega_n^{(m)}t} \phi(\lambda, 0) - \int_0^t e^{\Omega_n^{(m)}(s-t)} (\partial_s \phi(\lambda, s)) ds \right) \\ \implies \left| \int_0^t e^{\Omega_n^{(m)}(s-t)} \phi(\lambda, s) ds \right| &= \mathcal{O}(|k|^{-2}) \end{aligned}$$

uniformly in $\arg(k)^2$, as $k \rightarrow \infty$ within $\mathbb{C}^+ \setminus \mathcal{D}_m^+$, since the eigenvalues are directly proportional to k^2 . Therefore, the term in the square brackets of each of $T_2^{(m)}(x, t; 1)$ and $T_3^{(m)}(x, t; 2)$ decays like $\mathcal{O}(k^{-1})$. Given also that the only singularity, at $k = 0$, is removable, the integrals along the contour of $\mathbb{C}^+ \setminus \mathcal{D}_m^+$ equal zero by Jordan's lemma and Cauchy's residue theorem. Therefore, we can deform their integration contours from $+\mathbb{R}$ to $\partial\mathcal{D}_m^+$. By a similar argument and using Jordan's lemma for the lower complex plane, the integration contour of $T_3^{(m)}(x, t; 1)$ and $T_4^{(m)}(x, t; 2)$ can be deformed from $-\mathbb{R}$ to $\partial\mathcal{D}_m^-$. We also deform $\partial\mathcal{D}_m^+$ to ∂D_m^+ and $\partial\mathcal{D}_m^-$ to ∂D_m^- . The reasons and justifications for this second deformation are given in §2.3.1 and §2.3.2. Consequently, we have achieved the Ehrenpreis form:

$$2\pi h(x, t) = \begin{cases} T_1(x, t; 1) + I_2^{(2)}(x, t; 1) - I_2^{(1)}(x, t; 1) + I_3^{(2)}(x, t; 1) - I_3^{(1)}(x, t; 1), & x \in (-1, L], \\ T_1(x, t; 2) + I_3^{(2)}(x, t; 2) - I_3^{(1)}(x, t; 2) + I_4^{(2)}(x, t; 2) - I_4^{(1)}(x, t; 2), & x \in (L, 1), \end{cases} \quad (2.2.9)$$

where $T_1(x, t; n)$ is the same as in (2.2.7) and

$$\begin{aligned} I_2^{(m)}(x, t; 1) &= \int_{\partial D_m^+} \text{Integrand of } T_2^{(m)}(x, t; 1), \\ I_3^{(m)}(x, t; 1) &= \int_{\partial D_m^-} \text{Integrand of } T_3^{(m)}(x, t; 1), \\ I_3^{(m)}(x, t; 2) &= \int_{\partial D_m^+} \text{Integrand of } T_3^{(m)}(x, t; 2), \\ I_4^{(m)}(x, t; 2) &= \int_{\partial D_m^-} \text{Integrand of } T_4^{(m)}(x, t; 2). \end{aligned}$$

²In this case, we specified the modulus of each function, as well as uniformity with respect to $\arg(k)$. In general, however, these may be unwritten since our \mathcal{O} follows the definition in [14, §3.2], and has both uniformity and the modulus inherent to its definition.

2.3 Stage 2

Standard UTM procedure requires a Dirichlet-to-Neumann map which involves finding expressions for each of the 32 spectral functions that appear in the Ehrenpreis form (2.2.9):

$$\begin{aligned}
& \boxed{u_0^{(m)}(k; 1, -1)}, \quad u_0^{(m)}(k; 1, L), \quad u_0^{(m)}(k; 2, L), \quad u_0^{(m)}(k; 2, 1), \\
& \boxed{u_1^{(m)}(k; 1, -1)}, \quad u_1^{(m)}(k; 1, L), \quad u_1^{(m)}(k; 2, L), \quad u_1^{(m)}(k; 2, 1), \\
& u_2^{(m)}(k; 1, -1), \quad u_2^{(m)}(k; 1, L), \quad u_2^{(m)}(k; 2, L), \quad \boxed{u_2^{(m)}(k; 2, 1)}, \\
& u_3^{(m)}(k; 1, -1), \quad u_3^{(m)}(k; 1, L), \quad u_3^{(m)}(k; 2, L), \quad \boxed{u_3^{(m)}(k; 2, 1)}, \quad m = 1, 2.
\end{aligned}$$

We temporarily drop all explicit t -dependence of the terms for simplicity of notation and because they are unimportant for our analysis in Stage 2. The spectral inhomogeneity $\tilde{P}^{(m)}$ is known because the inhomogeneity p is (assumed to be) known. Given our boundary conditions (2.1.2), the boxed spectral functions are also known. Therefore, there remain 24 unknown spectral functions for which we need to solve.

Let us rewrite our global relations (2.2.5) as

$$\begin{aligned}
& -e^{-iLk} \left(k^3 u_0^{(m)} - ik^2 u_1^{(m)} - k u_2^{(m)} + i u_3^{(m)} + \frac{i}{\mu S_1} \tilde{P}^{(m)} \right) (k; 1, L) \\
& + e^{ik} \left(-k u_2^{(m)} + i u_3^{(m)} \right) (k; 1, -1) \\
& = e^{ik} \left(-k^3 u_0^{(m)} + ik^2 u_1^{(m)} - \frac{i}{\mu S_1} \tilde{P}^{(m)} \right) (k; 1, -1) - K_1^{(m)}, \\
& e^{-iLk} \left(k^3 u_0^{(m)} - ik^2 u_1^{(m)} - k u_2^{(m)} + i u_3^{(m)} + \frac{i}{\mu S_2} \tilde{P}^{(m)} \right) (k; 2, L) \\
& + e^{-ik} \left(-k^3 u_0^{(m)} + ik^2 u_1^{(m)} \right) (k; 2, 1) \\
& = e^{-ik} \left(-k u_2^{(m)} + i u_3^{(m)} + \frac{i}{\mu S_2} \tilde{P}^{(m)} \right) (k; 2, 1) - K_2^{(m)}, \tag{2.3.1}
\end{aligned}$$

where

$$K_1^{(m)} = \frac{1}{\mu S_1} \left(\Omega_1^{(m)} \hat{h}_0 - \hat{g}_0 + e^{\Omega_1^{(m)} t} \left(\hat{g} - \Omega_1^{(m)} \hat{h} \right) \right) (k; 1),$$

$$K_2^{(m)} = \frac{1}{\mu S_2} \left(\Omega_2^{(m)} \hat{h}_0 - \hat{g}_0 + e^{\Omega_2^{(m)} t} \left(\hat{g} - \Omega_2^{(m)} \hat{h} \right) \right) (k; 2),$$

for $m = 1, 2$. The right and left hand side of each equation in (2.3.1) contains the known and unknown spectral functions respectively. The functions \hat{h} and \hat{g} are treated as known functions for we will later show that they do not contribute to the solution. All other functions are known. In each K term, the arguments $(k; 1)$ and $(k; 2)$ only pertain to the functions $\hat{h}_0, \hat{g}_0, \hat{h}, \hat{g}$. The argument of each eigenvalue $\Omega_n^{(m)}$, while unwritten, will always be k . The significance of this will be made clear later when we apply maps of k .

Let us examine the symmetries of the dispersion relation and solve

$$\det (\Lambda_n(\nu(k)) - \Omega_n^{(m)}(k)I) = 0, \quad n(x) = 1, 2, \quad m = 1, 2,$$

for $\nu(k)$. We have the trivial solution: k and the invariance solution: $-k$. In addition, by considering the permutations of the eigenvalue indices, n and m , we can find the solutions that interchange index m : $\pm ik$, as well as the solutions that interchange index n , and the solutions that interchange both indices n and m . Consequently, we have the eight maps

$$k \mapsto k, \quad k \mapsto -k, \quad k \mapsto \begin{cases} \left(\frac{S_2}{S_1} \right)^{\frac{1}{4}} k, & n(x) = 1, \\ \left(\frac{S_1}{S_2} \right)^{\frac{1}{4}} k, & n(x) = 2, \end{cases} \quad k \mapsto \begin{cases} - \left(\frac{S_2}{S_1} \right)^{\frac{1}{4}} k, & n(x) = 1, \\ - \left(\frac{S_1}{S_2} \right)^{\frac{1}{4}} k, & n(x) = 2, \end{cases}$$

$$k \mapsto ik, \quad k \mapsto -ik, \quad k \mapsto \begin{cases} \left(\frac{S_2}{S_1} \right)^{\frac{1}{4}} ik, & n(x) = 1, \\ \left(\frac{S_1}{S_2} \right)^{\frac{1}{4}} ik, & n(x) = 2, \end{cases} \quad k \mapsto \begin{cases} - \left(\frac{S_2}{S_1} \right)^{\frac{1}{4}} ik, & n(x) = 1, \\ - \left(\frac{S_1}{S_2} \right)^{\frac{1}{4}} ik, & n(x) = 2. \end{cases}$$

Given these eight maps, a naive approach is to apply every map to (2.3.1). This approach, however, will result in the appearance of eight superfluous unknown spectral boundary functions $u_2^{(m)}(k; 2, -1)$, $u_3^{(m)}(k; 2, -1)$, $u_0^{(m)}(k; 1, 1)$ and $u_1^{(m)}(k; 1, 1)$, for $m = 1, 2$. Although we can solve for these superfluous unknowns alongside the unknowns that appear in the Ehrenpreis form, it would require solving a larger system than necessary (we will have 32 equations and 32 unknowns). We propose an alternative approach that works for our present problem but may have limited generalisability; this method requires smoothness at the interface. We use maps that do not interchange index n to eliminate all unknown spectral boundary functions, then use the remaining maps to solve for the unknown spectral interface functions. There are many equivalent ways to accomplish this and we will only present one way.

First, apply $k \mapsto ik$ and divide throughout by i to get

$$\begin{aligned}
& -e^{Lk} \left(-k^3 u_0^{(m)} + k^2 u_1^{(m)} - k u_2^{(m)} + u_3^{(m)} + \frac{1}{\mu S_1} \tilde{P}^{(m)} \right) (k; 1, L) \\
& e^{-k} \left(-k u_2^{(m)} + u_3^{(m)} \right) (k; 1, -1) = e^{-k} \left(k^3 u_0^{(m)} - k^2 u_1^{(m)} - \frac{1}{\mu S_1} \tilde{P}^{(m)} \right) (k; 1, -1) + K_3^{(m)}, \\
& e^{Lk} \left(-k^3 u_0^{(m)} + k^2 u_1^{(m)} - k u_2^{(m)} + u_3^{(m)} + \frac{1}{\mu S_2} \tilde{P}^{(m)} \right) (k; 2, L) \\
& + e^k \left(k^3 u_0^{(m)} - k^2 u_1^{(m)} \right) (k; 2, 1) = e^k \left(-k u_2^{(m)} + u_3^{(m)} + \frac{1}{\mu S_2} \tilde{P}^{(m)} \right) (k; 2, 1) + K_4^{(m)}, \\
\\
& K_3^{(m)} = \frac{i}{\mu S_1} \left(\Omega_1^{(m)} \hat{h}_0 - \hat{g}_0 + e^{\Omega_1^{(m)} t} \left(\hat{g} - \Omega_1^{(m)} \hat{h} \right) \right) (ik; 1), \\
& K_4^{(m)} = \frac{i}{\mu S_2} \left(\Omega_2^{(m)} \hat{h}_0 - \hat{g}_0 + e^{\Omega_2^{(m)} t} \left(\hat{g} - \Omega_2^{(m)} \hat{h} \right) \right) (ik; 2). \tag{2.3.2a}
\end{aligned}$$

The effect of the map $k \mapsto ik$ on the eigenvalues is to swap their m -index, i.e. $\Omega_n^{(1)} \mapsto \Omega_n^{(2)}$ and $\Omega_n^{(2)} \mapsto \Omega_n^{(1)}$. The argument of each eigenvalue remains k

whereas the argument of each function $\hat{h}_0, \hat{g}_0, \hat{h}, \hat{g}$ is transformed accordingly.

This explains the forms of functions $K_3^{(m)}$ and $K_4^{(m)}$.

Next, apply $k \mapsto -ik$ and divide throughout by i to get

$$\begin{aligned}
& -e^{-Lk} \left(k^3 u_0^{(m)} + k^2 u_1^{(m)} + k u_2^{(m)} + u_3^{(m)} + \frac{1}{\mu S_1} \tilde{P}^{(m)} \right) (k; 1, L) \\
& e^k \left(k u_2^{(m)} + u_3^{(m)} \right) (k; 1, -1) = e^k \left(-k^3 u_0^{(m)} - k^2 u_1^{(m)} - \frac{1}{\mu S_1} \tilde{P}^{(m)} \right) (k; 1, -1) + K_5^{(m)}, \\
& e^{-Lk} \left(k^3 u_0^{(m)} + k^2 u_1^{(m)} + k u_2^{(m)} + u_3^{(m)} + \frac{1}{\mu S_2} \tilde{P}^{(m)} \right) (k; 2, L) \\
& + e^{-k} \left(-k^3 u_0^{(m)} - k^2 u_1^{(m)} \right) (k; 2, 1) = e^{-k} \left(k u_2^{(m)} + u_3^{(m)} + \frac{1}{\mu S_2} \tilde{P}^{(m)} \right) (k; 2, 1) + K_6^{(m)}, \\
\\
& K_5^{(m)} = \frac{i}{\mu S_1} \left(\Omega_1^{(m)} \hat{h}_0 - \hat{g}_0 + e^{\Omega_1^{(m)} t} \left(\hat{g} - \Omega_1^{(m)} \hat{h} \right) \right) (-ik; 1), \\
& K_6^{(m)} = \frac{i}{\mu S_2} \left(\Omega_2^{(m)} \hat{h}_0 - \hat{g}_0 + e^{\Omega_2^{(m)} t} \left(\hat{g} - \Omega_2^{(m)} \hat{h} \right) \right) (-ik; 2). \tag{2.3.2b}
\end{aligned}$$

We use (2.3.2a) and (2.3.2b) to solve for the eight unknown boundary spectral functions. In effect, we only have to solve two 2-by-2 systems because the equations are decoupled about the indices n and m . The equations are decoupled about m since we previously diagonalised $\Lambda_n(k)$ (see (2.2.2) to (2.2.4)). The decoupling about n stems from the fact that each set of global relations (2.2.5) pertains solely to one sub-interval. We get

$$\begin{aligned}
& \left(-k u_2^{(m)} + i u_3^{(m)} \right) (k; 1, -1) = \left(k^3 u_0^{(m)} - i k^2 u_1^{(m)} - \frac{i}{\mu S_1} \tilde{P}^{(m)} \right) (k; 1, -1) \\
& + (\sinh(k(L+1)) + i \cosh(k(L+1))) \left(k^2 u_1^{(m)} + u_3^{(m)} + \frac{1}{\mu S_1} \tilde{P}^{(m)} \right) (k; 1, L) \\
& - (i \sinh(k(L+1)) + \cosh(k(L+1))) \left(k^3 u_0^{(m)} + k u_2^{(m)} \right) (k; 1, L) \\
& + \frac{i+1}{2} e^k K_3^{(m)} + \frac{i-1}{2} e^{-k} K_5^{(m)}, \tag{2.3.3a}
\end{aligned}$$

and

$$\begin{aligned}
& \left(-k^3 u_0^{(m)} + ik^2 u_1^{(m)} \right) (k; 2, 1) = \left(k u_2^{(m)} - i u_3^{(m)} - \frac{i}{\mu S_2} \tilde{P}^{(m)} \right) (k; 2, 1) \\
& + (i \cosh(k(1-L)) - \sinh(k(1-L))) \left(k^2 u_1^{(m)} + u_3^{(m)} + \frac{1}{\mu S_2} \tilde{P}^{(m)} \right) (k; 2, L) \\
& + (\sinh(k(L+1)) + i \cosh(k(L+1))) \left(k^3 u_0^{(m)} + k u_2^{(m)} \right) (k; 2, L) \\
& + \frac{1-i}{2} e^k K_6^{(m)} - \frac{i+1}{2} e^{-k} K_4^{(m)}, \tag{2.3.3b}
\end{aligned}$$

both of which also appear in the Ehrenpreis form (2.2.9). Substitute (2.3.3a) and (2.3.3b) into (2.3.1) to attain

$$\begin{aligned}
& \left[k^3 \theta_1^- \quad k^2 \eta_1^+ \quad k \theta_1^+ \quad \eta_1^- \right] (k) \cdot \left[u_0^{(m)} \quad u_1^{(m)} \quad u_2^{(m)} \quad u_3^{(m)} \right] (k; 1, L) \\
& = 2e^{ik} \left(-k^3 u_0^{(m)} + ik^2 u_1^{(m)} \right) (k; 1, -1) - \frac{\eta_1^-(k)}{\mu S_1} \tilde{P}^{(m)}(k; 1, L) + K_7^{(m)}, \\
& \left[k^3 \theta_2^+ \quad k^2 \eta_2^- \quad k \theta_2^- \quad \eta_2^+ \right] (k) \cdot \left[u_0^{(m)} \quad u_1^{(m)} \quad u_2^{(m)} \quad u_3^{(m)} \right] (k; 2, L) \\
& = 2e^{-ik} \left(-k u_2^{(m)} + i u_3^{(m)} + \frac{i}{\mu S_2} \tilde{P}^{(m)} \right) (k; 2, 1) - \frac{\eta_2^+(k)}{\mu S_2} \tilde{P}^{(m)}(k; 2, L) + K_8^{(m)}, \tag{2.3.4a}
\end{aligned}$$

which is written as a dot product so that the coefficients of the spectral interface functions may be easily extracted. We define

$$\begin{aligned}
\theta_1^\pm(k) &= \pm e^{-iLk} - \frac{1}{2} e^{ik} \left((1+i) e^{k(L+1)} + (1-i) e^{-k(L+1)} \right), \\
\eta_1^\pm(k) &= \pm i e^{-iLk} + \frac{1}{2} e^{ik} \left((1+i) e^{k(L+1)} - (1-i) e^{-k(L+1)} \right), \\
\theta_2^\pm(k) &= \pm e^{-iLk} + \frac{1}{2} e^{-ik} \left((i-1) e^{k(1-L)} - (1+i) e^{-k(1-L)} \right), \\
\eta_2^\pm(k) &= \pm i e^{-iLk} + \frac{1}{2} e^{-ik} \left((i-1) e^{k(1-L)} + (1+i) e^{-k(1-L)} \right), \tag{2.3.5}
\end{aligned}$$

$$\begin{aligned}
K_7^{(m)} &= \frac{1}{2\mu S_1} \left[e^{k(1+i)} (i-1) \left(\hat{g}_0 - \Omega_1^{(m)} \hat{h}_0 + e^{\Omega_1^{(m)} t} \left(\Omega_1^{(m)} \hat{h} - \hat{g} \right) \right) (ik; 1) \right. \\
&\quad - e^{k(i-1)} (1+i) \left(\hat{g}_0 - \Omega_1^{(m)} \hat{h}_0 + e^{\Omega_1^{(m)} t} \left(\Omega_1^{(m)} \hat{h} - \hat{g} \right) \right) (-ik; 1) \\
&\quad \left. + 2 \left(\hat{g}_0 - \Omega_1^{(m)} \hat{h}_0 + e^{\Omega_1^{(m)} t} \left(\Omega_1^{(m)} \hat{h} - \hat{g} \right) \right) (k; 1) \right], \\
K_8^{(m)} &= \frac{1}{2\mu S_2} \left[e^{k(1-i)} (1+i) \left(\hat{g}_0 - \Omega_2^{(m)} \hat{h}_0 + e^{\Omega_2^{(m)} t} \left(\Omega_2^{(m)} \hat{h} - \hat{g} \right) \right) (-ik; 2) \right. \\
&\quad - e^{-k(i+1)} (i-1) \left(\hat{g}_0 - \Omega_2^{(m)} \hat{h}_0 + e^{\Omega_2^{(m)} t} \left(\Omega_2^{(m)} \hat{h} - \hat{g} \right) \right) (ik; 2) \\
&\quad \left. + 2 \left(\hat{g}_0 - \Omega_2^{(m)} \hat{h}_0 + e^{\Omega_2^{(m)} t} \left(\Omega_2^{(m)} \hat{h} - \hat{g} \right) \right) (k; 2) \right].
\end{aligned}$$

Now apply three unused non-identity maps to (2.3.4a). From $k \mapsto -k$,

$$\begin{aligned}
&\left[-k^3 \theta_1^- \quad k^2 \eta_1^+ \quad -k \theta_1^+ \quad \eta_1^- \right] (-k) \cdot \left[u_0^{(m)} \quad u_1^{(m)} \quad u_2^{(m)} \quad u_3^{(m)} \right] (k; 1, L) \\
&= 2e^{-ik} \left(k^3 u_0^{(m)} + ik^2 u_1^{(m)} \right) (k; 1, -1) - \frac{\eta_1^-(-k)}{\mu S_1} \tilde{P}^{(m)}(k; 1, L) + K_9^{(m)}, \\
&\left[-k^3 \theta_2^+ \quad k^2 \eta_2^- \quad -k \theta_2^- \quad \eta_2^+ \right] (-k) \cdot \left[u_0^{(m)} \quad u_1^{(m)} \quad u_2^{(m)} \quad u_3^{(m)} \right] (k; 2, L) \\
&= 2e^{ik} \left(k u_2^{(m)} + i u_3^{(m)} + \frac{i}{\mu S_2} \tilde{P}^{(m)} \right) (k; 2, 1) - \frac{\eta_2^+(-k)}{\mu S_2} \tilde{P}^{(m)}(k; 2, L) + K_{10}^{(m)},
\end{aligned} \tag{2.3.4b}$$

where

$$\begin{aligned}
K_9^{(m)} &= \frac{1}{2\mu S_1} \left[e^{-k(1+i)} (i-1) \left(\hat{g}_0 - \Omega_1^{(m)} \hat{h}_0 + e^{\Omega_1^{(m)} t} \left(\Omega_1^{(m)} \hat{h} - \hat{g} \right) \right) (-ik; 1) \right. \\
&\quad - e^{k(1-i)} (1+i) \left(\hat{g}_0 - \Omega_1^{(m)} \hat{h}_0 + e^{\Omega_1^{(m)} t} \left(\Omega_1^{(m)} \hat{h} - \hat{g} \right) \right) (ik; 1) \\
&\quad \left. + 2 \left(\hat{g}_0 - \Omega_1^{(m)} \hat{h}_0 + e^{\Omega_1^{(m)} t} \left(\Omega_1^{(m)} \hat{h} - \hat{g} \right) \right) (-k; 1) \right], \\
K_{10}^{(m)} &= \frac{1}{2\mu S_2} \left[e^{k(i-1)} (1+i) \left(\hat{g}_0 - \Omega_2^{(m)} \hat{h}_0 + e^{\Omega_2^{(m)} t} \left(\Omega_2^{(m)} \hat{h} - \hat{g} \right) \right) (ik; 2) \right. \\
&\quad - e^{k(1+i)} (i-1) \left(\hat{g}_0 - \Omega_2^{(m)} \hat{h}_0 + e^{\Omega_2^{(m)} t} \left(\Omega_2^{(m)} \hat{h} - \hat{g} \right) \right) (-ik; 2) \\
&\quad \left. + 2 \left(\hat{g}_0 - \Omega_2^{(m)} \hat{h}_0 + e^{\Omega_2^{(m)} t} \left(\Omega_2^{(m)} \hat{h} - \hat{g} \right) \right) (-k; 2) \right].
\end{aligned}$$

From

$$k \mapsto \begin{cases} \left(\frac{S_2}{S_1}\right)^{\frac{1}{4}} k, & n(x) = 1, \\ \left(\frac{S_1}{S_2}\right)^{\frac{1}{4}} k, & n(x) = 2, \end{cases}$$

we get

$$\begin{aligned} & \left[\left(\frac{S_1}{S_2}\right)^{\frac{3}{4}} k^3 \theta_2^+ \quad \left(\frac{S_1}{S_2}\right)^{\frac{1}{2}} k^2 \eta_2^- \quad \left(\frac{S_1}{S_2}\right)^{\frac{1}{4}} k \theta_2^- \quad \eta_2^+ \right] \left(\left(\frac{S_1}{S_2}\right)^{\frac{1}{4}} k \right) \\ & \left[u_0^{(m)} \quad u_1^{(m)} \quad u_2^{(m)} \quad u_3^{(m)} \right] (k; 1, L) \\ & = 2e^{-i\left(\frac{S_1}{S_2}\right)^{\frac{1}{4}} k} \left(-\left(\frac{S_1}{S_2}\right)^{\frac{1}{4}} k u_2^{(m)} + i u_3^{(m)} + \frac{i}{\mu S_2} \tilde{P}^{(m)} \right) (k; 1, 1) \\ & - \frac{1}{\mu S_2} \eta_2^+ \left(\left(\frac{S_1}{S_2}\right)^{\frac{1}{4}} k \right) \tilde{P}^{(m)}(k; 1, L) + K_{11}^{(m)}, \\ & \left[\left(\frac{S_2}{S_1}\right)^{\frac{3}{4}} k^3 \theta_1^- \quad \left(\frac{S_2}{S_1}\right)^{\frac{1}{2}} k^2 \eta_1^+ \quad \left(\frac{S_2}{S_1}\right)^{\frac{1}{4}} k \theta_1^+ \quad \eta_1^- \right] \left(\left(\frac{S_2}{S_1}\right)^{\frac{1}{4}} k \right) \\ & \left[u_0^{(m)} \quad u_1^{(m)} \quad u_2^{(m)} \quad u_3^{(m)} \right] (k; 2, L) \\ & = 2e^{i\left(\frac{S_2}{S_1}\right)^{\frac{1}{4}} k} \left(-\left(\frac{S_2}{S_1}\right)^{\frac{3}{4}} k^3 u_0^{(m)} + i \left(\frac{S_2}{S_1}\right)^{\frac{1}{2}} k^2 u_1^{(m)} \right) (k; 2, -1) \\ & - \frac{1}{\mu S_1} \eta_1^- \left(\left(\frac{S_2}{S_1}\right)^{\frac{1}{4}} k \right) \tilde{P}^{(m)}(k; 2, L) + K_{12}^{(m)}, \end{aligned} \quad (2.3.4c)$$

where $K_{11}^{(m)}$ and $K_{12}^{(m)}$ are given by

$$\begin{aligned} & \frac{1}{2\mu S_2} \left[e^{\left(\frac{S_1}{S_2}\right)^{\frac{1}{4}} k(1-i)} (1+i) \left(\hat{g}_0 - \Omega_1^{(m)} \hat{h}_0 + e^{\Omega_1^{(m)} t} \left(\Omega_1^{(m)} \hat{h} - \hat{g} \right) \right) \left(-i \left(\frac{S_1}{S_2}\right)^{\frac{1}{4}} k; 2 \right) \right. \\ & \quad \left. - e^{-\left(\frac{S_1}{S_2}\right)^{\frac{1}{4}} k(i+1)} (i-1) \left(\hat{g}_0 - \Omega_1^{(m)} \hat{h}_0 + e^{\Omega_1^{(m)} t} \left(\Omega_1^{(m)} \hat{h} - \hat{g} \right) \right) \left(i \left(\frac{S_1}{S_2}\right)^{\frac{1}{4}} k; 2 \right) \right. \\ & \quad \left. + 2 \left(\hat{g}_0 - \Omega_1^{(m)} \hat{h}_0 + e^{\Omega_1^{(m)} t} \left(\Omega_1^{(m)} \hat{h} - \hat{g} \right) \right) \left(\left(\frac{S_1}{S_2}\right)^{\frac{1}{4}} k; 2 \right) \right], \end{aligned}$$

$$\begin{aligned} & \frac{1}{2\mu S_1} \left[e^{\left(\frac{S_2}{S_1}\right)^{\frac{1}{4}} k(1+i)} (i-1) \left(\hat{g}_0 - \Omega_2^{(m)} \hat{h}_0 + e^{\Omega_2^{(m)} t} \left(\Omega_2^{(m)} \hat{h} - \hat{g} \right) \right) \left(i \left(\frac{S_2}{S_1} \right)^{\frac{1}{4}} k; 1 \right) \right. \\ & \quad - e^{\left(\frac{S_2}{S_1}\right)^{\frac{1}{4}} k(i-1)} (1+i) \left(\hat{g}_0 - \Omega_2^{(m)} \hat{h}_0 + e^{\Omega_2^{(m)} t} \left(\Omega_2^{(m)} \hat{h} - \hat{g} \right) \right) \left(-i \left(\frac{S_2}{S_1} \right)^{\frac{1}{4}} k; 1 \right) \\ & \quad \left. + 2 \left(\hat{g}_0 - \Omega_2^{(m)} \hat{h}_0 + e^{\Omega_2^{(m)} t} \left(\Omega_2^{(m)} \hat{h} - \hat{g} \right) \right) \left(\left(\frac{S_2}{S_1} \right)^{\frac{1}{4}} k; 1 \right) \right], \end{aligned}$$

respectively. Note that the top equation of (2.3.4a) was mapped to the bottom equation of (2.3.4c) and vice versa. Accordingly, $K_7^{(m)}$ was mapped to $K_{12}^{(m)}$ and $K_8^{(m)}$ was mapped to $K_{11}^{(m)}$. From

$$k \mapsto \begin{cases} -\left(\frac{S_2}{S_1}\right)^{\frac{1}{4}} k, & n(x) = 1, \\ -\left(\frac{S_1}{S_2}\right)^{\frac{1}{4}} k, & n(x) = 2, \end{cases}$$

we get

$$\begin{aligned} & \left[-\left(\frac{S_1}{S_2}\right)^{\frac{3}{4}} k^3 \theta_2^+ \quad \left(\frac{S_1}{S_2}\right)^{\frac{1}{2}} k^2 \eta_2^- \quad -\left(\frac{S_1}{S_2}\right)^{\frac{1}{4}} k \theta_2^- \quad \eta_2^+ \right] \left(-\left(\frac{S_1}{S_2}\right)^{\frac{1}{4}} k \right) \\ & \left[u_0^{(m)} \quad u_1^{(m)} \quad u_2^{(m)} \quad u_3^{(m)} \right] (k; 1, L) \\ & = 2e^{i\left(\frac{S_1}{S_2}\right)^{\frac{1}{4}} k} \left(\left(\frac{S_1}{S_2}\right)^{\frac{1}{4}} k u_2^{(m)} + i u_3^{(m)} + \frac{i}{\mu S_2} \tilde{P}^{(m)} \right) (k; 1, 1) \\ & - \frac{1}{\mu S_2} \eta_2^+ \left(-\left(\frac{S_1}{S_2}\right)^{\frac{1}{4}} k \right) \tilde{P}^{(m)}(k; 1, L) + K_{13}^{(m)}, \\ & \left[-\left(\frac{S_2}{S_1}\right)^{\frac{3}{4}} k^3 \theta_1^- \quad \left(\frac{S_2}{S_1}\right)^{\frac{1}{2}} k^2 \eta_1^+ \quad -\left(\frac{S_2}{S_1}\right)^{\frac{1}{4}} k \theta_1^+ \quad \eta_1^- \right] \left(-\left(\frac{S_2}{S_1}\right)^{\frac{1}{4}} k \right) \\ & \left[u_0^{(m)} \quad u_1^{(m)} \quad u_2^{(m)} \quad u_3^{(m)} \right] (k; 2, L) \\ & = 2e^{-i\left(\frac{S_2}{S_1}\right)^{\frac{1}{4}} k} \left(\left(\frac{S_2}{S_1}\right)^{\frac{3}{4}} k^3 u_0^{(m)} + i \left(\frac{S_2}{S_1}\right)^{\frac{1}{2}} k^2 u_1^{(m)} \right) (k; 2, -1) \\ & - \frac{1}{\mu S_1} \eta_1^- \left(-\left(\frac{S_2}{S_1}\right)^{\frac{1}{4}} k \right) \tilde{P}^{(m)}(k; 2, L) + K_{14}^{(m)}, \end{aligned} \tag{2.3.4d}$$

where $K_{13}^{(m)}$ and $K_{14}^{(m)}$ are given by

$$\begin{aligned} & \frac{1}{2\mu S_2} \left[e^{\left(\frac{S_1}{S_2}\right)^{\frac{1}{4}} k(i-1)} (1+i) \left(\hat{g}_0 - \Omega_1^{(m)} \hat{h}_0 + e^{\Omega_1^{(m)} t} \left(\Omega_1^{(m)} \hat{h} - \hat{g} \right) \right) \left(i \left(\frac{S_1}{S_2} \right)^{\frac{1}{4}} k; 2 \right) \right. \\ & \quad - e^{\left(\frac{S_1}{S_2}\right)^{\frac{1}{4}} k(1+i)} (i-1) \left(\hat{g}_0 - \Omega_1^{(m)} \hat{h}_0 + e^{\Omega_1^{(m)} t} \left(\Omega_1^{(m)} \hat{h} - \hat{g} \right) \right) \left(-i \left(\frac{S_1}{S_2} \right)^{\frac{1}{4}} k; 2 \right) \\ & \quad \left. + 2 \left(\hat{g}_0 - \Omega_1^{(m)} \hat{h}_0 + e^{\Omega_1^{(m)} t} \left(\Omega_1^{(m)} \hat{h} - \hat{g} \right) \right) \left(- \left(\frac{S_1}{S_2} \right)^{\frac{1}{4}} k; 2 \right) \right], \\ & \frac{1}{2\mu S_1} \left[e^{-\left(\frac{S_2}{S_1}\right)^{\frac{1}{4}} k(1+i)} (i-1) \left(\hat{g}_0 - \Omega_2^{(m)} \hat{h}_0 + e^{\Omega_2^{(m)} t} \left(\Omega_2^{(m)} \hat{h} - \hat{g} \right) \right) \left(-i \left(\frac{S_2}{S_1} \right)^{\frac{1}{4}} k; 1 \right) \right. \\ & \quad - e^{\left(\frac{S_2}{S_1}\right)^{\frac{1}{4}} k(1-i)} (1+i) \left(\hat{g}_0 - \Omega_2^{(m)} \hat{h}_0 + e^{\Omega_2^{(m)} t} \left(\Omega_2^{(m)} \hat{h} - \hat{g} \right) \right) \left(i \left(\frac{S_2}{S_1} \right)^{\frac{1}{4}} k; 1 \right) \\ & \quad \left. + 2 \left(\hat{g}_0 - \Omega_2^{(m)} \hat{h}_0 + e^{\Omega_2^{(m)} t} \left(\Omega_2^{(m)} \hat{h} - \hat{g} \right) \right) \left(- \left(\frac{S_2}{S_1} \right)^{\frac{1}{4}} k; 1 \right) \right], \end{aligned}$$

respectively. Our boundary conditions (2.1.2) imply that $u_1(k; 1, -1) = u_2(k; 2, 1) = u_3(k; 2, 1) = 0$. In order to reduce the length of our expressions and increase readability, we encode (2.3.4a) as

$$\begin{aligned} a_0 u_0^{(m)}(k; 1, L) + a_1 u_1^{(m)}(k; 1, L) + a_2 u_2^{(m)}(k; 1, L) + a_3 u_3^{(m)}(k; 1, L) + a_4^{(m)} &= 0, \\ \alpha_0 u_0^{(m)}(k; 2, L) + \alpha_1 u_1^{(m)}(k; 2, L) + \alpha_2 u_2^{(m)}(k; 2, L) + \alpha_3 u_3^{(m)}(k; 2, L) + \alpha_4^{(m)} &= 0, \end{aligned}$$

where, making use of our boundary conditions,

$$\begin{aligned} a_4^{(m)} &= \frac{\tilde{P}^{(m)}(k; 1, L) \eta_1^-(k)}{S_1 \mu} + 2e^{ik} k^3 u_0^{(m)}(k; 1, -1) - K_7^{(m)}, \\ \alpha_4^{(m)} &= \frac{\tilde{P}^{(m)}(k; 2, L) \eta_2^+(k)}{S_2 \mu} - 2e^{-ik} \frac{i \tilde{P}^{(m)}}{S_2 \mu}(k; 2, 1) - K_8^{(m)}, \end{aligned}$$

and the coefficients can be taken directly from (2.3.4a). We use Latin and Greek letters for equations pertaining to $n(x) = 1$ and $n(x) = 2$ respectively.

We encode (2.3.4b), (2.3.4c), (2.3.4d) in the same way with

$$\begin{aligned}
b_4^{(m)} &= \frac{\tilde{P}^{(m)}(k; 1, L)\eta_1^-(-k)}{S_1\mu} - 2e^{-ik}k^3u_0^{(m)}(k; 1, -1) - K_9^{(m)}, \\
\beta_4^{(m)} &= \frac{\tilde{P}^{(m)}(k; 2, L)\eta_2^+(-k)}{S_2\mu} - 2e^{ik}\frac{i\tilde{P}^{(m)}}{S_2\mu}(k; 2, 1) - K_{10}^{(m)}, \\
c_4^{(m)} &= \frac{1}{\mu S_2}\eta_2^+\left(\left(\frac{S_1}{S_2}\right)^{\frac{1}{4}}k\right)\tilde{P}^{(m)}(k; 1, L) - 2e^{-i\left(\frac{S_1}{S_2}\right)^{\frac{1}{4}}k}\frac{i}{\mu S_2}\tilde{P}^{(m)}(k; 1, 1) - K_{11}^{(m)}, \\
\kappa_4^{(m)} &= \frac{1}{\mu S_1}\eta_1^-\left(\left(\frac{S_2}{S_1}\right)^{\frac{1}{4}}k\right)\tilde{P}^{(m)}(k; 2, L) + 2e^{i\left(\frac{S_2}{S_1}\right)^{\frac{1}{4}}k}\left(\frac{S_2}{S_1}\right)^{\frac{3}{4}}k^3u_0^{(m)}(k; 2, -1) - K_{12}^{(m)}, \\
d_4^{(m)} &= \frac{1}{\mu S_2}\eta_2^+\left(-\left(\frac{S_1}{S_2}\right)^{\frac{1}{4}}k\right)\tilde{P}^{(m)}(k; 1, L) - 2e^{i\left(\frac{S_1}{S_2}\right)^{\frac{1}{4}}k}\frac{i}{\mu S_2}\tilde{P}^{(m)}(k; 1, 1) - K_{13}^{(m)}, \\
\delta_4^{(m)} &= \frac{1}{\mu S_1}\eta_1^-\left(-\left(\frac{S_2}{S_1}\right)^{\frac{1}{4}}k\right)\tilde{P}^{(m)}(k; 2, L) \\
&\quad - 2e^{-i\left(\frac{S_2}{S_1}\right)^{\frac{1}{4}}k}\left(\frac{S_2}{S_1}\right)^{\frac{3}{4}}k^3u_0^{(m)}(k; 2, -1) - K_{14}^{(m)}. \tag{2.3.6}
\end{aligned}$$

We use (2.3.4a), (2.3.4b), (2.3.4c) and (2.3.4d) to solve for the 16 unknown spectral interface functions. Using Cramer's rule, we get the following expressions³ for $m = 1, 2$,

$$\begin{aligned}
u_0^{(m)}(k; 1, L) &= \frac{1}{\Delta_1(k)} \sum_{\ell qrs \in \text{Sym}(\{1,2,3,4\})} a_\ell^{(m)} b_q^{(m)} c_r^{(m)} d_s^{(m)}, \\
u_1^{(m)}(k; 1, L) &= \frac{1}{\Delta_1(k)} \sum_{\ell qrs \in \text{Sym}(\{0,2,3,4\})} a_\ell^{(m)} b_q^{(m)} c_r^{(m)} d_s^{(m)}, \\
u_2^{(m)}(k; 1, L) &= \frac{1}{\Delta_1(k)} \sum_{\ell qrs \in \text{Sym}(\{0,1,3,4\})} a_\ell^{(m)} b_q^{(m)} c_r^{(m)} d_s^{(m)}, \\
u_3^{(m)}(k; 1, L) &= \frac{1}{\Delta_1(k)} \sum_{\ell qrs \in \text{Sym}(\{0,1,2,4\})} a_\ell^{(m)} b_q^{(m)} c_r^{(m)} d_s^{(m)}, \\
\text{where } \Delta_1(k) &= \sum_{\ell qrs \in \text{Sym}(\{0,1,2,3\})} a_\ell b_q c_r d_s,
\end{aligned}$$

³Note that the expression $\ell qrs \in \text{Sym}(\{1, 2, 3, 4\})$ means “the permutation ℓqrs in the symmetric group of set $\{1, 2, 3, 4\}$ ”.

$$\begin{aligned}
u_0^{(m)}(k; 2, L) &= \frac{1}{\Delta_2(k)} \sum_{\ell qrs \in \text{Sym}(\{1,2,3,4\})} \alpha_\ell^{(m)} \beta_q^{(m)} \kappa_r^{(m)} \delta_s^{(m)}, \\
u_1^{(m)}(k; 2, L) &= \frac{1}{\Delta_2(k)} \sum_{\ell qrs \in \text{Sym}(\{0,2,3,4\})} \alpha_\ell^{(m)} \beta_q^{(m)} \kappa_r^{(m)} \delta_s^{(m)}, \\
u_2^{(m)}(k; 2, L) &= \frac{1}{\Delta_2(k)} \sum_{\ell qrs \in \text{Sym}(\{0,1,3,4\})} \alpha_\ell^{(m)} \beta_q^{(m)} \kappa_r^{(m)} \delta_s^{(m)}, \\
u_3^{(m)}(k; 2, L) &= \frac{1}{\Delta_2(k)} \sum_{\ell qrs \in \text{Sym}(\{0,1,2,4\})} \alpha_\ell^{(m)} \beta_q^{(m)} \kappa_r^{(m)} \delta_s^{(m)}, \\
\text{where } \Delta_2(k) &= \sum_{\ell qrs \in \text{Sym}(\{0,1,2,3\})} \alpha_\ell \beta_q \kappa_r \delta_s. \tag{2.3.7}
\end{aligned}$$

Finally, substitute these functions into (2.3.3a) and (2.3.3b) to attain expressions for $(-ku_2^{(m)} + iu_3^{(m)})(k; 1, -1)$ and $(k^3u_0^{(m)} - ik^2u_1^{(m)})(k; 2, 1)$ which appear in the Ehrenpreis form (2.2.9). Substituting every unknown spectral function in the Ehrenpreis form with the expressions we found almost gives the final solution representation. The spectral functions \hat{g} and \hat{h} in the eight terms $K_7^{(m)}$ to $K_{14}^{(m)}$ remain unknown. Thus, the final step of Stage 2 is to show that they do not contribute to the solution and can be removed.

2.3.1 Demonstrating zero contribution from each integral that contains \hat{g} and \hat{h}

Consider the Ehrenpreis form (2.2.9) with all the spectral functions substituted. Assume that we can distribute the integrals to isolate \hat{g} and \hat{h} . Then, to show that \hat{g} and \hat{h} do not contribute to the solution, we simply need to show that the integrals that contain \hat{g} and \hat{h} each equal zero. This would also provide post-hoc justification for the distribution of integrals. Examining the Ehrenpreis form and its constituent terms (see (2.2.9) and (2.2.7)), we can see that each distributed integral that contains \hat{g} and \hat{h} will

be of the form

$$\int_{\partial D_m^+} e^{ik\lambda} \phi(k) dk \quad \text{or} \quad \int_{\partial D_m^-} e^{-ik\lambda} \phi(k) dk,$$

where ϕ contains \hat{g} and \hat{h} , and $\lambda > 0$. We want to show that ϕ decays as $\arg(k) \rightarrow \infty$ within $\text{clos } D_m^+$ or $\text{clos } D_m^-$, depending on the integration contour. We also want to show that ϕ has no non-removable singularities in the same region. Then, by Jordan's lemma and Cauchy's theorem, the integral equals zero, as desired. Within this argument lies the reason for our contour deformations in Stage 1. If we had not deformed the integration contours from \mathbb{R} , our regions of interest would be $\text{clos } \mathbb{C}^\pm$ instead of $\text{clos } D_m^\pm$. It is usually impossible to make the argument for $\text{clos } \mathbb{C}^\pm$.

In our case, our regions of interest are $\text{clos } D_1^+$, $\text{clos } D_2^+$, $\text{clos } D_1^-$, $\text{clos } D_2^-$. These are, in order, subsets of the quadrants of \mathbb{C} . Thus, it should be possible for us to make the argument for $\text{clos } \mathbb{C}^\pm$. Nonetheless, the argument is much easier if we consider one quadrant at a time.

Definition 1. Define $\mathcal{C} = \{\text{clos } D_1^+, \text{clos } D_1^-, \text{clos } D_2^+, \text{clos } D_2^-\}$ (see (2.2.8) for the definition of each region of interest). In addition, define $Z(\phi) = \{k \in \mathbb{C} : \phi(k)\phi(ik)\phi(-k)\phi(-ik) = 0\}$.

Our other challenge is to address the complex zeros of some functions in the Ehrenpreis form (2.2.9). The integrands in the Ehrenpreis form are entire by Morera's theorem. Once we distribute the integrals, however, each distributed integrand may have singularities due to the zeros of $\Delta_n(k)$. These singularities impede our Jordan-lemma-Cauchy-theorem argument. In addition, our asymptotic analysis requires certain functions to be sufficiently far from their zeros; these functions are exponential polynomials

and will be specified in the proceeding theorems. We want there to exist $M \in \mathbb{R}^+$ such that for each of these functions ϕ , $|\phi(k)| \geq M > 0$ for all $k \in \bigcup \mathcal{C}$; assume that $M \ll 1$. We accomplish this by having the set of complex zeros and its rotations $Z(\phi) \subseteq \Xi$, and we preemptively remove an open disc around each zero. The removal of the open discs poses its own challenges though, and we will discuss the removal in §2.3.2.

Definition 2. For complex functions ϕ, ψ , define $\phi = \mathcal{O}_\ell(\psi)$ as $\phi = \mathcal{O}(\psi)$ uniformly in $\arg(k)$, as $k \rightarrow \infty$ within C , where $C \in \mathcal{C}$ and C is a subset of the closure of the ℓ th quadrant of \mathbb{C} . We define Θ_ℓ and o_ℓ analogously⁴.

Lemma 3. Define $\theta_1 = \{\theta_1^+, \theta_1^-, \eta_1^+, \eta_1^-\}$ and $\theta_2 = \{\theta_2^+, \theta_2^-, \eta_2^+, \eta_2^-\}$ (see (2.3.5) for the definition of each function). For every ϕ in

$$\left\{ (1+i)e^{k(L+1)} + (1-i)e^{-k(L+1)}, (1+i)e^{k(L+1)} - (1-i)e^{-k(L+1)}, \right. \\ \left. (i-1)e^{k(1-L)} - (1+i)e^{-k(1-L)}, (i-1)e^{k(1-L)} + (1+i)e^{-k(1-L)} \right\} \cup \theta_1 \cup \theta_2,$$

let $Z(\phi) \subseteq \Xi$. Then, for all $\varphi \in \theta_1$ and $\psi \in \theta_2$,

$$\begin{aligned} \text{for } L \in (-1, 0], \varphi(k) &= \Theta_1(e^{-iLk} + e^{ik}e^{k(L+1)}), \Theta_2(e^{-iLk} + e^{ik}e^{-k(L+1)}), \\ &\quad \Theta_3(e^{ik}e^{-k(L+1)}), \Theta_4(e^{ik}e^{k(L+1)}), \\ \psi(k) &= \Theta_1(e^{-ik}e^{k(1-L)}), \Theta_2(e^{-ik}e^{-k(1-L)}), \\ &\quad \Theta_3(e^{-iLk} + e^{-ik}e^{-k(1-L)}), \Theta_4(e^{-iLk} + e^{-ik}e^{k(1-L)}), \\ \text{for } L \in (0, 1), \varphi(k) &= \Theta_1(e^{-iLk} + e^{ik}e^{k(L+1)}), \Theta_2(e^{-iLk} + e^{ik}e^{-k(L+1)}), \\ &\quad \Theta_3(e^{ik}e^{-k(L+1)}), \Theta_4(e^{ik}e^{k(L+1)}), \end{aligned}$$

⁴Our Θ follows Knuth's definition [8], except that, like for \mathcal{O} in [14, §3.2], we automatically add a modulus around each function that is being compared since it is complex. We have that $(\phi = \mathcal{O}(\psi) \text{ and } \psi = \mathcal{O}(\phi)) \iff \phi = \Theta(\psi) \iff \psi = \Theta(\phi)$; Θ is an equivalence relation. As for o , we use the standard definition except with the modulus.

$$\begin{aligned}\psi(k) = & \Theta_1(e^{-ik}e^{k(1-L)}), \Theta_2(e^{-ik}e^{-k(1-L)}), \\ & \Theta_3(e^{-iLk} + e^{-ik}e^{-k(1-L)}), \Theta_4(e^{-iLk} + e^{-ik}e^{k(1-L)}).\end{aligned}$$

Proof. Since $L \in (-1, 1)$, $L + 1 > 0$ and $1 - L > 0$. Refer to Table 2.1 for the asymptotic behaviour of basic exponential functions in each complex quadrant. If $L \in (-1, 0]$, it is immediately apparent from Table 2.1 that $|\theta_1^\pm(k)|, |\eta_1^\pm(k)|$ all behave like $\Theta_3(e^{ik}e^{-k(L+1)})$ and $\Theta_4(e^{ik}e^{k(L+1)})$. In addition, the functions behave like $\Theta(e^{-iLk})$ if $\text{Im}(k) \rightarrow \infty$ and $\text{Re}(k)$ is bounded, and like $\Theta(e^{ik}e^{\pm k(L+1)})$ if $\text{Re}(k) \rightarrow \pm\infty$ and $\text{Im}(k)$ is bounded.

Now consider $k \rightarrow \infty$ in the first quadrant with $\text{Re}(k)$ and $\text{Im}(k)$ unbounded. When $\text{Re}(k)$ is large, the ratio of the magnitude of any two functions in θ_1 can be approximately expressed as

$$\frac{|F(k)e^{-iLk} - \frac{1}{2}(1+i)e^{ik}(e^{k(L+1)})|}{|G(k)e^{-iLk} + \frac{1}{2}(1+i)e^{ik}(e^{k(L+1)})|},$$

where F, G are functions such that $|F(k)| = |G(k)| = 1$. This ratio is bounded above by

$$\frac{|(F(k) + G(k))e^{-iLk} - M|}{M} \leq \frac{(|F(k)| + |G(k)|)|e^{-iLk}| + M}{M} \leq \frac{2 + M}{M},$$

and bounded below by

$$\frac{M}{|(F(k) + G(k))e^{-iLk} - M|} \geq \frac{M}{(|F(k)| + |G(k)|)|e^{-iLk}| + M} \geq \frac{M}{2 + M},$$

since $e^{-iLk} = o_1(1)$. If $|k|$ is large but $\text{Re}(k)$ is small, then $\text{Im}(k)$ is large. In that case the dominant term in each of $\theta_1^\pm(k), \eta_1^\pm(k)$ is e^{-iLk} . We may analyse $|\theta_1^\pm(k)|, |\eta_1^\pm(k)|$ further to find that they are asymptotically bounded

above and below by real functions $e^{(L+1)z}$ and e^{Lz} respectively, for $z > 0$, though they may oscillate infinitely between these bounds. This behaviour is tangential to the statement of the lemma though. The proof for the second quadrant highly similar: interchange $e^{k(L+1)}$ with $e^{-k(L+1)}$. Through similar analysis and with reference to Table 2.1, we can determine the asymptotic behaviour of the functions in θ_2 .

Next, we consider $L \in (0, 1)$. The proof is highly similar and in many ways symmetric to what we have above. We can immediately conclude that $|\theta_2^\pm(k)|$, $|\eta_2^\pm(k)|$ behave like $\Theta_1(e^{k(1-L)}e^{-ik})$ and $\Theta_2(e^{-k(1-L)}e^{-ik})$. In addition, the functions in θ_2 behave like $\Theta(e^{-iLk})$ if $\text{Im}(k) \rightarrow -\infty$ and $\text{Re}(k)$ is bounded, and like $\Theta(e^{-ik}e^{\pm k(L+1)})$ if $\text{Re}(k) \rightarrow \pm\infty$ and $\text{Im}(k)$ is bounded. Consider $k \rightarrow \infty$ in the fourth quadrant with $\text{Re}(k)$ and $\text{Im}(k)$ unbounded. When $\text{Re}(k)$ is large, the ratio of the magnitude of any two functions in θ_2 can be approximately expressed as

$$\frac{|F(k)e^{-iLk} + \frac{1}{2}(i-1)e^{-ik}(e^{k(L+1)})|}{|G(k)e^{-iLk} + \frac{1}{2}(i-1)e^{-ik}(e^{k(L+1)})|},$$

where F, G are functions such that $|F(k)| = |G(k)| = 1$. As for θ_1 above, this ratio is bounded above and below by

$$\frac{|(F(k) - G(k))e^{-iLk} + M|}{M} \leq \frac{2 + M}{M}, \text{ and}$$

$$\frac{M}{|(G(k) - F(k))e^{-iLk} + M|} \geq \frac{M}{2 + M}$$

respectively since $e^{-iLk} = o_3(1)$. If $|k|$ is large but $\text{Re}(k)$ is small, then $\text{Im}(k)$ is large. In that case the dominant term in each of θ_2^\pm, η_2^\pm is e^{-iLk} . The proof for the third quadrant is similar. Through analysis similar to that presented above, we can determine the asymptotic behaviour of the

If $k \rightarrow \infty$ within:	Decay	Blow-up
D_1^+ (1st quadrant)	e^{-k}, e^{ik}	e^k, e^{-ik}
D_2^+ (2nd quadrant)	e^k, e^{ik}	e^{-k}, e^{-ik}
D_1^- (3rd quadrant)	e^k, e^{-ik}	e^{-k}, e^{ik}
D_2^- (4th quadrant)	e^{-k}, e^{-ik}	e^k, e^{ik}

TABLE 2.1: The asymptotic behaviour of basic exponential functions as $k \rightarrow \infty$ in a subset of each quadrant of \mathbb{C} .

functions in θ_1 as well to conclude our proof. \square

Corollary 4. *Let $Z(\Delta_1), Z(\Delta_2), Z(a_\ell b_q c_r d_s), Z(\alpha_\ell \beta_q \kappa_r \delta_s) \subseteq \Xi$ for all $\ell q r s \in \text{Sym}(\{1, 2, 3, 4\})$ (see (2.3.7) for definitions). Then, $\{a_\ell b_q c_r d_s : \ell q r s \in \text{Sym}(\{1, 2, 3, 4\})\} \cup \{\Delta_1\}$ and $\{\alpha_\ell \beta_q \kappa_r \delta_s : \ell q r s \in \text{Sym}(\{1, 2, 3, 4\})\} \cup \{\Delta_2\}$ are each a Θ_l equivalence class for $l = 1, 2, 3, 4$.*

Proof. Observe that for all $\ell q r s \in \text{Sym}(\{1, 2, 3, 4\})$,

$$a_\ell b_q c_r d_s = k^6 \phi_1(k) \psi_1(-k) \phi_2 \left(\left(\frac{S_1}{S_2} \right)^{\frac{1}{4}} k \right) \psi_2 \left(- \left(\frac{S_1}{S_2} \right)^{\frac{1}{4}} k \right),$$

$$\alpha_\ell \beta_q \kappa_r \delta_s = k^6 \Phi_2(k) \Psi_2(-k) \Phi_1 \left(\left(\frac{S_1}{S_2} \right)^{\frac{1}{4}} k \right) \Psi_1 \left(- \left(\frac{S_1}{S_2} \right)^{\frac{1}{4}} k \right),$$

for some $\phi_1, \psi_1, \Phi_1, \Psi_1 \in \theta_1$ and $\phi_2, \psi_2, \Phi_2, \Psi_2 \in \theta_2$. Lemma 3 implies that θ_1, θ_2 are each a Θ_ℓ equivalence class for $\ell = 1, 2, 3, 4$. Therefore,

$$a_\ell b_q c_r d_s = \Theta_\ell \left[k^6 \theta_1^+(k) \theta_1^+(-k) \theta_2^+ \left(\left(\frac{S_1}{S_2} \right)^{\frac{1}{4}} k \right) \theta_2^+ \left(- \left(\frac{S_1}{S_2} \right)^{\frac{1}{4}} k \right) \right],$$

$$\alpha_\ell \beta_q \kappa_r \delta_s = \Theta_\ell \left[k^6 \theta_2^+(k) \theta_2^+(-k) \theta_1^+ \left(\left(\frac{S_1}{S_2} \right)^{\frac{1}{4}} k \right) \theta_1^+ \left(- \left(\frac{S_1}{S_2} \right)^{\frac{1}{4}} k \right) \right].$$

Clearly Δ_1 and Δ_2 will each behave like their constituent terms. \square

Observe from (2.3.6) that $K_7^{(m)}$ only appears in the term $a_4^{(m)}$. Therefore, the coefficient of $K_7^{(m)}$ in $u_0^{(m)}(k; 1, L)$ has magnitude

$$\left| \frac{1}{\Delta_1(k)} \sum_{qrs \in \text{Sym}(\{1,2,3\})} b_q c_r d_s \right| \leq \frac{1}{|\Delta_1(k)|} \sum_{qrs \in \text{Sym}(\{1,2,3\})} |b_q c_r d_s|.$$

Corollary 4 implies that for k in each region $C \in \mathcal{C}$, and for each $\ell qrs \in \text{Sym}(\{0, 1, 2, 3\})$, there exists some positive constant $F_{\ell qrs}$ such that $|\Delta_1(k)| \geq F_{\ell qrs} |a_\ell b_q c_r d_s|$ for $|k|$ sufficiently large. Therefore, we have that

$$\begin{aligned} |\Delta_1(k)| &\geq |a_0| \sum_{qrs \in \text{Sym}(\{1,2,3\})} F_{0qrs} |b_q c_r d_s| \\ &\geq |a_0| \min_{qrs \in \text{Sym}(\{1,2,3\})} (F_{0qrs}) \sum_{qrs \in \text{Sym}(\{1,2,3\})} |b_q c_r d_s|. \end{aligned}$$

This implies that $\exists F > 0$ such that for $k \in C \in \mathcal{C}$ and $|k|$ sufficiently large,

$$\left| \frac{1}{\Delta_1(k)} \sum_{qrs \in \text{Sym}(\{1,2,3\})} b_q c_r d_s \right| \leq \frac{1}{F} \left| \frac{1}{a_0} \right|,$$

which implies that the coefficient behaves like $\mathcal{O}_\ell(1/a_0)$ for $\ell = 1, 2, 3, 4$. Examination of the coefficients of the spectral interface functions in (2.3.4a) reveals that $k^3 a_0$, $k^2 a_1$, $k a_2$, and a_3 have the same asymptotic behaviour, which is $\mathcal{O}_\ell(1/\theta_1^+(k))$. Through similar methods, we determine that the coefficient of each of $K_7^{(m)}$ to $K_{14}^{(m)}$ in the spectral functions behaves like

$$\begin{aligned} K_7^{(m)} &: \mathcal{O}_\ell \left(\frac{1}{\theta_1^+(k)} \right), & K_8^{(m)} &: \mathcal{O}_\ell \left(\frac{1}{\theta_2^+(k)} \right), \\ K_9^{(m)} &: \mathcal{O}_\ell \left(\frac{1}{\theta_1^+(-k)} \right), & K_{10}^{(m)} &: \mathcal{O}_\ell \left(\frac{1}{\theta_2^+(-k)} \right), \\ K_{11}^{(m)} &: \mathcal{O}_\ell \left(1 / \theta_2^+ \left(\left(\frac{S_1}{S_2} \right)^{\frac{1}{4}} k \right) \right), & K_{12}^{(m)} &: \mathcal{O}_\ell \left(1 / \theta_1^+ \left(\left(\frac{S_2}{S_1} \right)^{\frac{1}{4}} k \right) \right), \end{aligned}$$

$$K_{13}^{(m)} : \mathcal{O}_\ell \left(1 / \theta_2^+ \left(- \left(\frac{S_1}{S_2} \right)^{\frac{1}{4}} k \right) \right), \quad K_{14}^{(m)} : \mathcal{O}_\ell \left(1 / \theta_1^+ \left(- \left(\frac{S_2}{S_1} \right)^{\frac{1}{4}} k \right) \right), \quad (2.3.8)$$

for $\ell = 1, 2, 3, 4$. Next, consider the definitions of $\hat{h}(k; 1)$ and $\hat{h}(k; 2)$ in (2.2.6a). Perform integration by parts to get

$$\begin{aligned} \hat{h}(k; 1) &= \frac{i}{k} (e^{-iLk}h(L) - e^{ik}h(-1)) + \frac{i}{k} \int_{-1}^L e^{-ikx}h_x(x)dx, \\ \hat{h}(k; 2) &= \frac{i}{k} (e^{-ik}h(1) - e^{-iLk}h(L)) + \frac{i}{k} \int_L^1 e^{-ikx}h_x(x)dx. \end{aligned}$$

Recall that $L \in (-1, 1)$. We re-express the integrals as

$$\begin{aligned} \int_{-1}^L e^{-ikx}h_x(x)dx &= \begin{cases} e^{-iLk} \int_{-1}^L e^{-ik(x-L)}h_x(x)dx, & \text{if } k \in \text{clos } \mathbb{C}^+, \\ e^{ik} \int_{-1}^L e^{-ik(x+1)}h_x(x)dx, & \text{if } k \in \mathbb{C}^-, \end{cases} \\ \int_L^1 e^{-ikx}h_x(x)dx &= \begin{cases} e^{-ik} \int_L^1 e^{-ik(x-1)}h_x(x)dx, & \text{if } k \in \text{clos } \mathbb{C}^+, \\ e^{-iLk} \int_L^1 e^{-ik(x-L)}h_x(x)dx, & \text{if } k \in \mathbb{C}^-. \end{cases} \end{aligned}$$

The asymptotic behaviour of the integrals in the various cases are $o(1)$ by the Riemann–Lebesgue lemma. The solution function h is necessarily bounded.

Therefore, with reference to Table 2.1, we conclude that for $L \in (-1, 1)$,

$$\begin{aligned} \hat{h}(k; 1) &= \mathcal{O}_1 \left(\frac{e^{-iLk}}{k} \right), \mathcal{O}_2 \left(\frac{e^{-iLk}}{k} \right), \mathcal{O}_3 \left(\frac{e^{ik}}{k} \right), \mathcal{O}_4 \left(\frac{e^{ik}}{k} \right), \\ \hat{h}(k; 2) &= \mathcal{O}_1 \left(\frac{e^{-ik}}{k} \right), \mathcal{O}_2 \left(\frac{e^{-ik}}{k} \right), \mathcal{O}_3 \left(\frac{e^{-iLk}}{k} \right), \mathcal{O}_4 \left(\frac{e^{-iLk}}{k} \right). \quad (2.3.9) \end{aligned}$$

This holds even if $h(-1)$, $h(L)$ or $h(1)$ equals zero since a smaller integration interval will not change our upper bound. By the same analysis and

given that g is also bounded, $\hat{g}(k; 1)$ and $\hat{g}(k; 2)$ have the same asymptotic behaviour as $\hat{h}(k; 1)$ and $\hat{h}(k; 2)$ respectively.

Finally, we consider the three terms in each of $K_7^{(m)}$ and $K_8^{(m)}$ that contain \hat{h} . We ignore the factors $e^{\Omega_n^{(m)} t} \Omega_n^{(m)}$ because they will be cancelled out upon substitution into the Ehrenpreis form (see (2.2.9) and (2.2.7)). The asymptotic behaviours of $\hat{h}(k; 1)$ and $\hat{h}(k; 2)$ are given by (2.3.9). For the remaining four terms, we use (2.3.9) and the fact that the regions D_m^\pm have 4-fold rotational symmetry about the origin to get

$$\begin{aligned}
e^{k(i-1)} \hat{h}(-ik; 1) &= \mathcal{O}_2 \left(\frac{e^{-(L+1)k} e^{ik}}{k} \right), \mathcal{O}_3 \left(\frac{e^{-(L+1)k} e^{ik}}{k} \right), \mathcal{O}_4 \left(\frac{e^{ik}}{k} \right), \mathcal{O}_1 \left(\frac{e^{ik}}{k} \right), \\
e^{k(1+i)} \hat{h}(ik; 1) &= \mathcal{O}_4 \left(\frac{e^{(L+1)k} e^{ik}}{k} \right), \mathcal{O}_1 \left(\frac{e^{(L+1)k} e^{ik}}{k} \right), \mathcal{O}_2 \left(\frac{e^{ik}}{k} \right), \mathcal{O}_3 \left(\frac{e^{ik}}{k} \right), \\
e^{k(1-i)} \hat{h}(-ik; 2) &= \mathcal{O}_2 \left(\frac{e^{-ik}}{k} \right), \mathcal{O}_3 \left(\frac{e^{-ik}}{k} \right), \mathcal{O}_4 \left(\frac{e^{(1-L)k} e^{-ik}}{k} \right), \mathcal{O}_1 \left(\frac{e^{(1-L)k} e^{-ik}}{k} \right), \\
e^{-k(i+1)} \hat{h}(ik; 2) &= \mathcal{O}_4 \left(\frac{e^{-ik}}{k} \right), \mathcal{O}_1 \left(\frac{e^{-ik}}{k} \right), \mathcal{O}_2 \left(\frac{e^{-(1-L)k} e^{-ik}}{k} \right), \mathcal{O}_3 \left(\frac{e^{-(1-L)k} e^{-ik}}{k} \right).
\end{aligned} \tag{2.3.10}$$

From (2.3.8), the coefficients of $K_7^{(m)}$ and $K_8^{(m)}$ behave like $\mathcal{O}_\ell(1/\theta_1^+(k))$ and $\mathcal{O}_\ell(1/\theta_2^+(k))$ respectively. Compare the asymptotic behaviours given by lemma 3 with those given by (2.3.9) and (2.3.10). We conclude that the terms that contain \hat{h} in $K_7^{(m)}$ and $K_8^{(m)}$ all decay like $\mathcal{O}_\ell(k^{-1})$ upon substitution into the Ehrenpreis form, for $\ell = 1, 2, 3, 4$. Since \hat{g} lacks a factor of $\Omega_n^{(m)} \propto k^2$ compared to \hat{h} , the terms that contain \hat{g} in $K_7^{(m)}$ and $K_8^{(m)}$ decay like $\mathcal{O}_\ell(k^{-3})$. We repeat this analysis with $K_9^{(m)}$ to $K_{14}^{(m)}$ and find that every term that contains \hat{h} or \hat{g} in the Ehrenpreis form decays. This completes our Jordan-lemma-Cauchy-theorem argument. Eliminating \hat{h} and \hat{g} from each of $K_7^{(m)}$ to $K_{14}^{(m)}$ gives the final solution representation.

We have achieved a model of the kinematics with minimal assumptions. The UTM usually includes a Stage 3 to verify that the solution satisfies the problem, but we will omit it due to space constraints. Nonetheless, we will include a short section to justify the removal of the open discs.

2.3.2 Justifying the removal of the open discs

At the end of Stage 1, we preemptively removed an open disc $R(\xi, M)$ around each zero (and its rotations) of the exponential polynomials specified in lemma 3 and corollary 4. We constructed every open disc with some fixed radius M . This, however, may result in us attempting to remove an infinite region from \mathcal{D}_m^\pm in (2.2.8), which would require a Jordan-lemma-Cauchy-theorem argument similar to those used to justify the contour deformations. Fortunately, we have from [10] that the zeros of our exponential polynomials are isolated, so we can construct and remove such open discs.

Suppose we remove $R(\xi, M)$ around some $\xi \in \mathcal{D}_m^\pm$. Then, we will need to consider integrals over $\partial R(\xi, M)$ with integrands that contain $e^{-\Omega_n^{(m)}t}$. If ξ is at infinity, then our definitions of the regions (2.2.8) imply that $e^{-\Omega_n^{(m)}t}$, and consequently the integral, will diverge. This is especially problematic since Ξ is countably infinite. Thus, we require the zeros to asymptotically approach the real or imaginary axis as $e^{-\Omega_n^{(m)}t}$ is bounded along the axes.

Langer [9, Theorem 8] provides an elegant method to approximate the asymptotic location of the zeros of complex exponential polynomials. First, collect the power of each exponential term and take its conjugate. Next, plot the conjugate powers on the complex plane and construct a convex hull around the resultant shape. The zeros at infinity are confined “to a finite number of strips each of asymptotically constant width”, and the strips are

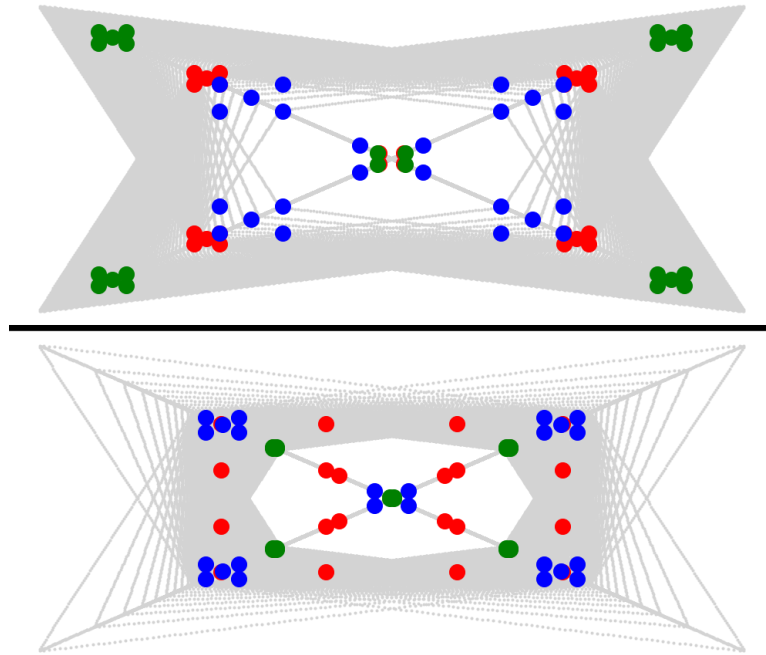


FIGURE 2.2: Each colour indicates a set of conjugate powers collected from $\Delta_1(k)$ (top) or $\Delta_2(k)$ (bottom), after cancellation with the numerator, for particular values of S_1/S_2 and L . Observe that the convex hull for each of these sets of points is rectangular. The points in grey show the conjugate powers for $S_1/S_2 \in [0.2, 5]$ and $L \in (-1, 1)$.

asymptotically perpendicular to a side of the convex hull. In our case, for $L \in (-1, 1)$ and $S_1, S_2 \in \mathbb{R}^+$, the convex hull is always a rectangle (see Figure 2.2 and our online appendix⁵). Unfortunately, this is insufficient since we require there to be exactly one strip centered on each axis with a width that converges to zero. Nonetheless, Langer's method can be paired with numerical analysis to demonstrate that the zeros behave as desired. Locating the zeros of exponential polynomials for a general UTM procedure remains an open problem in the literature. Mathematicians have had to employ ad hoc analytic methods (see [11] for another example; it also uses results from [9]) and/or numerical analysis.

⁵The Jupyter Notebook can be found here: <https://tinyurl.com/capstoneDH>.

Chapter 3

Further Analysis

In this final chapter, we will discuss the applications of our kinematics model to the flapping plate/fish tail problem. Our UTM-produced model has two unique strengths. First, every integral in the solution representation (2.2.9) converges uniformly [11, p. 4]. Second, the Jordan-lemma-Cauchy-theorem argument remains a powerful analytic tool.

Let us consider the question of whether the kinematics are simple harmonic. If there exists some positive constant F such that $h = -Fh_{tt}$, then h is simple harmonic. This approach requires that we determine h_{tt} . First, note that $\tilde{P}^{(m)}$, $u_0^{(m)}$, $u_1^{(m)}$, $u_2^{(m)}$, $u_3^{(m)}$ multiplied by $e^{-\Omega_n^{(m)}t}$ and with integration bounds (t, \mathcal{T}) instead of $(0, t)$ (see (2.2.6b) for definitions), each has the form $\int_t^{\mathcal{T}} e^{\Omega_n^{(m)}(s-t)} \phi(\lambda, s) ds$. Integration by parts gives

$$\begin{aligned} \int_t^{\mathcal{T}} e^{\Omega_n^{(m)}(s-t)} \phi(\lambda, s) ds &= \frac{1}{\Omega_n^{(m)}} \left(e^{\Omega_n^{(m)}(\mathcal{T}-t)} \phi(\lambda, \mathcal{T}) - \phi(\lambda, t) \right. \\ &\quad \left. - \int_t^{\mathcal{T}} e^{\Omega_n^{(m)}(s-t)} (\partial_s \phi(\lambda, s)) ds \right) \implies \left| \int_t^{\mathcal{T}} e^{\Omega_n^{(m)}(s-t)} \phi(\lambda, s) ds \right| = \mathcal{O}(k^{-2}) \end{aligned}$$

as $k \rightarrow \infty$ within $\text{clos } \mathcal{D}_m^+$. Through the same arguments as for the contour deformations, we can replace the integration bound in each term with $(0, \mathcal{T})$. With this change, the t -dependence in the solution representation comes

solely from the exponential factors $e^{-\Omega_n^{(m)}t}$. Given uniform convergence, twice differentiating h with respect to t simply multiplies each integrand by $(\Omega_n^{(m)})^2 = -(\mu S_n)k^4$. The resultant integrals are difficult to evaluate, but no more difficult than the originals. If the integrals that pertain to each interval (see (2.2.9)), evaluates to the same limit but with a factor of $1/S_1$ or $1/S_2$ respectively, despite its integrand having been multiplied by k^4 , then h is simple harmonic with $F = \mu$. Relatedly, we can examine the accuracy of the approximation by considering $\min_{F \in \mathbb{R}^+} \|Fh + h_{tt}\|$.

If $h_0 \equiv g_0 \equiv 0$, we do not expect $h(x, 1/\omega) = g(x, 1/\omega) = 0$, where ω is the frequency of the driver. In fact, a characteristic of hyperbolic PDEs is that perturbations propagate at finite speed [4, §2.3]. Thus, another approach is to hypothesise that $h = H + o(t)$, where H is simple harmonic and the remainder converges uniformly in x . We expect at least some component of our initial condition to be in the remainder. Yet, a Jordan-lemma-Cauchy-theorem argument will not work since $e^{-\Omega_n^{(m)}t}$ diverges as $k \rightarrow \infty$ in D_m^\pm . In fact, for t sufficiently large, $e^{-\Omega_n^{(m)}t}$ will overpower any decay in the other exponential terms since their powers are bounded.

Lastly, we consider S_2/S_1 large and $L \rightarrow -1$ which, by Moore's hypothesis, should result in maximum thrust. Observe then that in D_m^\pm , either

$$2e^{i\left(\frac{S_2}{S_1}\right)^{\frac{1}{4}}k} \left(\frac{S_2}{S_1}\right)^{\frac{3}{4}} k^3 u_0^{(m)}(k; 2, -1) \quad \text{or} \quad -2e^{-i\left(\frac{S_2}{S_1}\right)^{\frac{1}{4}}k} \left(\frac{S_2}{S_1}\right)^{\frac{3}{4}} k^3 u_0^{(m)}(k; 2, -1)$$

from $\kappa_4^{(m)}$ and $\delta_4^{(m)}$ (2.3.6) respectively, both of which pertain to $n(x) = 2$, will be dominant. This is especially true upon substitution into the Ehrenpreis form (2.2.9). Since $u_0^{(m)}(k; 2, -1)$ represents the driver, this result may indicate that these parameters maximise the effect of the driver on the kinematics which results in maximal generation of thrust.

Bibliography

- [1] Naga Praveen Babu Mannam, Md. Mahbub Alam, and P. Krishnankutty, *Review of biomimetic flexible flapping foil propulsion systems on different planetary bodies*, Results in Engineering **8** (2020), 1–19.
- [2] B. Deconinck, N. E. Sheils, and D. A. Smith, *The linear KdV equation with an interface*, Comm. Math. Phys. **347** (2016), 489–509.
- [3] Bernard Deconinck, Guo Qi, Eli Shlizerman, and Vishal Vasan, *Fokas’s unified transform method for linear systems*, Quarterly of Applied Mathematics **76** (2018), 463–488.
- [4] James F. Doyle, *Flexural waves in beams*, pp. 88 – 125, Springer US, New York, NY, 1989.
- [5] A. S. Fokas, *A unified transform method for solving linear and certain non-linear PDEs*, Proc. R. Soc. Lond. Ser. A Math. Phys. Eng. Sci. **453** (1997), 1411–1443.
- [6] A. S. Fokas and B. Pelloni, *A transform method for linear evolution PDEs on a finite interval*, IMA J. Appl. Math. **70** (2005), 564–587.
- [7] Seon M. Han, Haym Benaroya, and Timothy Wei, *Dynamics of transversely vibrating beams using four engineering theories*, Journal of Sound and Vibration **255** (1999), 935–988.
- [8] D. Knuth, *Big omicron and big omega and big theta*, Sigact News **8** (1976), 18–24.

-
- [9] R. E. Langer, *On the zeros of exponential sums and integrals*, Bulletin of the American Mathematical Society **37** (1931), 213–239.
- [10] B. Ja. Levin, *Distributions of zeros of entire functions*, Translations of Mathematical Monographs, vol. 5, American Mathematical Society, Providence, Rhode Island, 1964.
- [11] P. D. Miller and D. A. Smith, *The diffusion equation with nonlocal data*, J. Math. Anal. Appl. **466** (2018), no. 2, 1119–1143.
- [12] M. Nicholas J. Moore, *Analytical results on the role of flexibility in flapping propulsion*, Journal of Fluid Mechanics **757** (2014), 599–612.
- [13] ———, *Torsional spring is the optimal flexibility arrangement for thrust production of a flapping wing*, Physics of Fluids **27** (2015), 1–7.
- [14] F.W.J. Olver, *Asymptotics and special functions*, Computer science and applied mathematics : a series of monographs and textbooks, Academic Press, 1974.
- [15] N.E. Sheils and B. Deconinck, *Interface problems for dispersive equations*, Studies in Applied Mathematics **134** (2015), no. 3, 253–275.
- [16] T. Yao-Tsu Wu, *Swimming of a waving plate*, Journal of Fluid Mechanics **10** (1961), 321–344.